The Effects of Physical Processes on the Hadley Circulation

DAVID RIND AND WILLIAM B. ROSSOW

NASA Goddard Space Flight Center, Institute for Space Studies, New York, NY 10025

(Manuscript received 8 June 1983, in final form 7 November 1983)

ABSTRACT

The Hadley cell is involved in the energy, momentum and moisture budgets in the atmosphere; it may be expected to change as sources and sinks of these quantities are altered due to climate perturbations. The nature of the Hadley cell change is complicated since alterations in one budget generally result in alterations in the others. Thus, Hadley cell sensitivity needs to be explored in an interactive system. In the GISS GCM (model I), a number of experiments are performed in which physical processes in each of the three budgets are omitted, the system adjusts, and the resultant circulation is compared to that of the control run. This procedure highlights which effects are most important and reveals the nature of the various interactions.

The results emphasize the wide variety of processes that appear capable of influencing the mean circulation. The intensity of the circulation is related to the coherence of the thermal forcing, and to the thermal opacity of the atmosphere. When all frictional forcing is removed, the circulation is restricted to the equatorial region. The latitudinal extent appears to be controlled primarily by eddy processes (Ferrel cell intensity). The implications for climate modeling and climate projections (e.g., rainfall changes) are discussed.

1. Introduction

The Hadley circulation is of central importance to the distribution of climate regimes on Earth and to the determination of atmospheric dynamics on other planets. Some scenarios, which envision the northward expansion of the subtropical arid zones into the breadbasket regions of the United States and the Soviet Union in response to climate warming by increasing CO_2 abundance (Manabe and Wetherald, 1980), in effect hypothesize the poleward expansion of the Hadley circulation subsidence regions. This change in the circulation, though small, would have important consequences for human societies. Hadley circulations on slowly rotating planets like Venus are presumed to stretch from equator to pole, while those on rapidly rotating planets like Jupiter are presumed to be confined close to the equator. These large differences in the meridional extent of Hadley circulations are attributed to the differences in planetary rotation rate (Hunt, 1979; Williams and Holloway, 1982), but they may also depend on other atmospheric processes, particularly large-scale eddy transports (Rossow, 1983). Understanding the sensitivity of Hadley-type circulation characteristics to alterations, both large and small, of atmospheric processes depends on understanding which processes influence the meridional circulation most.

In general, previous studies of the Hadley cell can be divided into two categories: 1) simple balance models with a few fixed physical processes and a limited range of potential feedbacks, and 2) general circulation models, with many processes and feedbacks but a limited range of experiments (usually one). The limitation of the first approach is that it fails to allow for atmospheric adjustments which may alter the effect of specified forcing, producing misleading estimates of sensitivity. The ability of the atmosphere to limit or amplify its response to perturbations is the major uncertainty in climate change assessments and cannot be ignored in the investigation of the Hadley cell's response to changing physical processes. The second approach simulates at least some of the complexity of the real circulation, but the limited number of experiments prevents diagnosis of the processes causing the adjustments of the circulation. In this paper we will report on a wide range of experiments that have been conducted with the GISS general circulation model. The procedure is to remove various physical processes, allow the circulation to adjust, and compare the result with that of a control run. Our aim is to highlight the influence of these processes within an interactive system. In addition to contributing to our understanding of the Hadley cell, this procedure should help isolate the aspects of the climate system which need to be modeled accurately in order to allow us to determine

the change in the mean circulation likely to arise with climate perturbations.

The Hadley circulation on Earth reacts to several different stimuli and accomplishes several different purposes. It transports geopotential energy produced partially by excess solar radiation poleward, angular momentum associated with the faster rotation of lower latitudes poleward and upward, and moisture away from the subtropical regions of high evaporation. The mean circulation actually transports sensible heat and moisture to the equator, generating more convection and mean vertical motion, both of which lift air. The lift provides the geopotential energy which is advected poleward by the mean circulation. Any physical process in a climate change scenario which affects the budgets of energy, momentum or moisture might be expected to influence the intensity and extent of the Hadley cell. We examine the question of what controls the sensitivity of Hadley circulations to changes in these three budgets, with special emphasis on the role of large-scale eddies. The sensitivity displayed by the model Hadley circulation may not be precisely that of Earth's Hadley circulation, but the perturbations introduced are sufficiently extreme that the gross nature of the response should be realistic. The model results emphasize the highly interactive nature of the various components of the system; it is likely that the real atmosphere is even more complex.

2. Analysis

The influence of different heat, momentum and moisture budget processes on the mean meridional circulation (MMC) can be illustrated by deriving an equation for the zonal mean streamfunction from the equations of zonal flow and energy (in Cartesian and pressure coordinates):

$$\frac{\partial \bar{u}}{\partial t} + \bar{v}\frac{\partial \bar{u}}{\partial y} + \bar{\omega}\frac{\partial \bar{u}}{\partial p} - f\bar{v} = -\bar{F}_x + \bar{L}, \quad (1)$$

$$\frac{\partial \bar{\Phi}_p}{\partial t} + \bar{v}\frac{\partial \bar{\Phi}_p}{\partial y} + \bar{\omega}\frac{\partial \bar{\Phi}_p}{\partial p} + \sigma\bar{\omega} = -\left(\frac{\kappa}{p}\right)\bar{H} - \bar{G}, \quad (2)$$

where $\bar{u}$, $\bar{v}$ and $\bar{\omega}$ are the zonally averaged wind speeds in the x, y, p directions, $\kappa = R/C_p$, R is the gas constant, C_p the specific heat at constant pressure, and $\sigma = -(\alpha/\bar{\theta})(\partial\bar{\theta}/\partial p)$ is the static stability parameter with α the specific volume and $\bar{\theta}$ the potential temperature. The vertical geopotential gradient is given by the hydrostatic relationship

$$\bar{\Phi}_p \equiv \frac{\partial \bar{\Phi}}{\partial p} = -\frac{R\bar{T}}{p}.$$

The remaining terms in (1) and (2) are $\bar{F}_x$, the momentum source-sink (friction) term,

$$\bar{F}_x = \bar{F}_x \text{ (surface friction)} + \bar{F}_x \text{ (cumulus friction)} + \bar{F}_x \text{ (mountain drag)},$$

$\bar{H}$, the heating rate term,

$$\bar{H} = \bar{H} \text{ (radiation)} + \bar{H} \text{ (sensible heat flux)} + \bar{H} \text{ (large scale condensation)} + \bar{H} \text{ (cumulus heating)},$$

$$\bar{H} \text{ (cumulus heating)} = \bar{H} \text{ (dry convective heating)} + \bar{H} \text{ (moist convective heating)} + \bar{H} \text{ (convective condensation)},$$

$$\bar{L} = -\frac{\partial}{\partial y}(\overline{u'v'}) - \frac{\partial}{\partial p}(\overline{u'\omega'}),$$

eddy momentum flux convergence,

$$\bar{G} = -\frac{\partial}{\partial y}(\overline{v'\Phi'_p}) - \frac{\partial}{\partial p}(\overline{\omega'\Phi'_p}),$$

eddy heat flux convergence.

Note that the commonly used form in (2) is an approximation obtained by assuming a base state vertical temperature profile $T_0(p)$ such that $\bar{T}(y, p, t) = T_0(p) + T^*(y, p, t)$. If the static stability of the base state is large compared with deviations in the static stability, i.e., $\sigma = \sigma_0 + \sigma^*$ and $\sigma_0 \gg |\sigma^*|$, then (2) results with $\bar{\Phi}_p = -RT^*/p$ (see, for example, Holton, 1975, p. 32). This approximation is equivalent to overestimating the smaller (by assumption) component of the dynamic heat fluxes that results from perturbations of the base state temperature. This component of the flux cannot be neglected for situations where $\sigma \approx 0$; but for most atmospheric models, some kind of convective adjustment is employed to avoid neutral stability for the large-scale dynamics, so that for the sake of discussion, the needed correction term can be considered part of $\bar{H}$ (cumulus heating).

The continuity equation in pressure coordinates defines a streamfunction for the zonally averaged circulation such that $\bar{v} = -\partial\psi/\partial p$ and $\bar{\omega} = \partial\psi/\partial y$. If (1) is differentiated by p and multiplied by f/σ, (2) is differentiated by y and divided by σ, and the results added, we get

$$-\left(\frac{\partial^2\psi}{\partial y^2} + \frac{f^2}{\sigma}\frac{\partial^2\psi}{\partial p^2}\right) = -\nabla^2_*\psi$$
$$= \frac{\kappa}{\sigma p}\frac{\partial \bar{H}}{\partial y} + \frac{1}{\sigma}\frac{\partial}{\partial y}\left(\frac{\partial \bar{\Phi}_p}{\partial t} + \bar{v}\frac{\partial \bar{\Phi}_p}{\partial y} + \bar{\omega}\frac{\partial \bar{\Phi}_p}{\partial p}\right)$$
$$+ \frac{1}{\sigma}\frac{\partial \bar{G}}{\partial y} + \frac{f}{\sigma}\frac{\partial \bar{F}_x}{\partial p} + \frac{f}{\sigma}\frac{\partial}{\partial p} \times \left(\frac{\partial \bar{u}}{\partial t} + v\frac{\partial \bar{u}}{\partial y} + \bar{\omega}\frac{\partial \bar{u}}{\partial p}\right) - \frac{f}{\sigma}\frac{\partial \bar{L}}{\partial p}. \quad (3)$$

With the approximate geometrical interpretation that the Laplacian (∇^2_*) of a variable is proportional to the negative of that variable, the left-hand side of (3) is

proportional to ψ. Thus, when the forcing terms on the right are negative, they force a (Northern Hemisphere) direct meridional circulation (negative ψ) with rising motion to the south, northward motion aloft, sinking motion nearer the North Pole, and southward motion below the circulation center. Positive forcing implies indirect circulation (positive ψ).

The first three terms on the right in (3) represent generation of ψ by radiative and other diabatic heat sources, by advection of heat by the MMC, and by eddy heat transports. The first of these is the direct thermal forcing which causes a Hadley circulation when the heating decreases with increasing latitude. Contributions to this term come from radiation, sensible heat flux from the surface (including small-scale turbulent transports), parameterized convective heat transports (dry and moist convection), and water vapor condensation (large and small scale). The second term represents the feedback on the directly forced MMC caused by the heat transport by the MMC itself. In quasi-geostrophic flow, this term represents forcing when the MMC alters the temperature field away from perfect geostrophic balance with the mean zonal wind; for example, a Hadley circulation is intensified when its winds are maximum at the location of the surface temperature maximum (for the typical January distribution of temperature). The third term intensifies Hadley circulations when eddy heat flux convergence, like diabatic heating, decreases with increasing latitude.

The last three terms on the right in (3) represent generation of ψ by "friction" processes, by advection of zonal momentum by the MMC, and by eddy momentum transports. The fourth term is the direct frictional forcing provided by surface drag, mountain drag and cumulus friction (or small-scale turbulent momentum mixing). These processes intensify Hadley circulations when they decrease with increasing altitude in an east wind regime as is the case with surface drag and cumulus friction in the tropics. The fifth term is the feedback on the forced circulation caused by MMC transport of angular momentum. This term represents forcing when the MMC momentum advection alters the mean zonal wind away from perfect geostrophic balance with the temperature field; for example, a Hadley circulation is intensified if $\partial\bar{u}/\partial y > 0$ in the Northern Hemisphere where $\partial\bar{u}/\partial p < 0$. The sixth term indicates that a Hadley circulation is intensified if eddy momentum flux convergence decreases with increasing altitude like surface drag or cumulus friction.

The hydrological cycle on Earth plays a key role in complicating the response of the MMC to perturbations by coupling several of the forcing terms in (3). The moisture budget can be written (l is the latent heat constant)

$$\bar{H}\ (\text{large scale condensation}) + \bar{H}\ (\text{convective condensation})$$
$$= -l\left(\frac{\partial\bar{q}}{\partial t} + \bar{v}\frac{\partial\bar{q}}{\partial y} + \bar{\omega}\frac{\partial\bar{q}}{\partial p}\right) + l\ (\text{evaporation}) + l\ (\text{eddy vapor flux convergence}) + l\ (\text{convective vapor flux convergence}). \quad (4)$$

In other words, the diabatic heating produced by cloud and precipitation formation is controlled by vapor flux convergence by the MMC, the large-scale eddies and convective (turbulent) motions [first, third and fourth terms on the right, in (4), respectively]. These terms therefore provide additional feedbacks between atmospheric motions and their effects on the MMC. The hydrological cycle also provides an implicit coupling between the heat and momentum forcing through the role of moist convection, since penetrative convection redistributes both heat and momentum forcing near the surface into the interior of the troposphere.

These equations thus contain forcing by thermal and frictional effects, eddy transfers of heat and momentum, and interactions due to water vapor. The contributions of the various processes have been estimated, generally using somewhat simplified forms of these equations. Eliassen (1951) investigated the forcing (i.e., evolution) of the mean circulation in a hydrostatic, geostrophic, circular vortex flow using linearized equations of motion [see also Kuo (1956) and in isentropic coordinates Gallimore and Johnson (1981)]. Point sources of heat and momentum produce distorted dipole-like streamfunctions; the orientation of the dipole axis is perpendicular to isentropes for a heat source and perpendicular to lines of constant angular momentum for an angular momentum source. Each type of source function drives only one wind component in its immediate vicinity: heating drives vertical motions and torques drive meridional motions. As we illustrate with the model, this result is equivalent to the requirement for both types of forcing to produce the complete circulation. The form of Eliassen's equations is similar to (3) and shows that stronger vertical motions are caused by heat sources more strongly confined in latitude, whereas stronger meridional motions are caused by angular momentum sources more strongly confined in altitude. In addition, the aspect ratio of the closed streamlines of the forced MMC depends on the relative stability of the vortex flow in the two coordinate directions. Low static stability leads to a larger vertical extent of the circulation, whereas low inertial stability leads to a larger meridional extent. Consequently, while the horizontal distribution of heating controls circulation intensity, its vertical distribution influences the vertical extent of the circulation. Likewise, while the vertical distribution of angular momentum sources controls circulation intensity, its horizontal distribution influences the horizontal extent of the circulation.

For a *steady* forced circulation, the sources of heat and momentum cannot be independently specified

(Gilman, 1964). For the zonal wind to be nearly independent of time, the rate of change of temperature must be similarly small. With a steady zonal wind the meridional wind is determined by the Coriolis torque necessary to balance momentum input against frictional removal; with a steady temperature field the vertical wind produces the adiabatic cooling necessary to balance nonadiabatic heat sources. As the zonally averaged meridional and vertical winds are associated through the equation of continuity, the total momentum and heat sources must be similarly associated. This is accomplished by the parts of the thermal and frictional forcing that are "internal" to the system. The most obvious such components are the surface frictional forcing, which is a function of the surface wind field, and the longwave cooling which is a function of the temperature field. In actuality, there is really no part of the system which is completely external: the absorbed solar radiation depends upon the cloud cover, which will react to changes in the temperature and moisture fields, and eddy forcing depends on the baroclinicity of the background state.

These relationships emphasize the fact that the forcing for the real Hadley circulation is not fixed, externally specified heating/cooling and friction. One example is the net heating of the atmosphere at low latitudes which exists in part because of energy transport by the circulation; without dynamic transport the temperature would rise until radiative balance (no net heating) is attained. All other forcing processes, especially the large-scale eddies, are similarly reactive when considered as the net forcing in a balanced circulation.

Various simplified models of the MMC have been studied to determine the processes which control the Hadley circulation characteristics. Schneider and Lindzen (1977) and Schoeberl and Strobel (1978) considered models which neglect all momentum and heat advection by the mean and eddy circulations in (3), except for vertical heat advection by the mean circulation with a specified static stability [the fourth term on the left in (2)]; i.e., (3) is reduced to

$$-\nabla_*^2\psi = \frac{f}{\sigma}\frac{\partial \bar{F}_x}{\partial p} + \frac{\kappa}{\sigma p}\frac{\partial \bar{H}}{\partial y}. \tag{5}$$

The MMC obtained in these models is simply the linear sum of the circulations produced by the specified forcing, which is usually fixed; the MMC cannot, in effect, alter the forcing magnitude. This approach is useful for studying the circulation forced directly by various individual ("external") processes, but it cannot be used to determine the *sensitivity* of the actual circulation because the feedbacks of the MMC on the forcing, in particular, the interactions between the MMC and large-scale eddies, are neglected. Some other studies include some of these feedbacks through parameterizations of other contributions to $\bar{F}_x$, $\bar{H}$, $\bar{L}$ and $\bar{G}$ (e.g., Hunt, 1973; Taylor, 1980; Held and Hou, 1980), but many other feedbacks and interactions, particularly between different processes, are neglected.

Dickinson (1971) attempted to determine the proper relative contributions of thermal and momentum sources to the steady mean circulation by explicitly dividing the forcing in a linear equatorial β-plane model into a "reactive" part in terms of Rayleigh friction and Newtonian cooling and the remaining sources of heat and momentum which are independently specified. These fixed "external" sources consisted of tropical rainbelt latent heat release, and horizontal eddy momentum fluxes. His results depended upon the assumed momentum and temperature damping rates: if the momentum damping rate is small compared to that of temperature, the meridional circulation is largely controlled by the distribution of the momentum sources, and if momentum is damped at a much greater rate, the circulation is controlled largely by the distribution of heat sources. In his study the conclusion was that the tropical rain belt by itself is sufficient to drive the observed Hadley cell, given the assumed damping rates. This process predominates because of the inefficient forcing due to solar radiation (Kuo, 1956) which is minimized by its input "near" the lower boundary with a constraint of vanishing vertical velocity there (Dickinson, 1971). As shown by our results even these "external" sources cannot be considered truly independent of the response of the system.

One very important example of this interdependence is the effect of a change in moisture availability. Such a change will affect $\bar{H}$ (condensation) directly, but the associated change in convective activity will also alter cumulus friction, $\bar{F}_x$, and eddy kinetic energy generation which, in turn, alters $\bar{L}$ and $\bar{G}$. In addition, changes in associated cloudiness and water vapor abundance alter both the solar and longwave components of $\bar{H}$ (radiation). Finally, the MMC and eddy contributions to $\bar{H}$ (condensation) are also changed. Hydrological processes form an interlocking set, all of which adjust to climate perturbations and feedback on each other.

Understanding the sensitivity of climate features dependent on the Ferrel circulation may present even more of a challenge. Diagnostic studies suggest that the Ferrel circulation is driven by both heat and momentum flux convergences (which as noted here cannot be independent) by large-scale eddies (Kuo, 1956; Vernekar, 1967; Crawford and Sasamori, 1981; Pfeffer, 1981). Moisture transport by eddies also plays a significant role in this case (Salustri and Stone, 1983). We will illustrate here that proper determination of the sensitivity of the MMC, both Hadley and Ferrel components, to climate changes requires accounting for the complex interactions of eddy transports and hydrological processes, which have been neglected in most previous studies of MMC sensitivity.

3. Model and experiments

The general circulation model used for these studies was developed over the past few years at the NASA Goddard Institute for Space Studies. The model is global with realistic topography. Important differences between this model and some others are that it calculates its own cloud cover and it uses no explicit horizontal or vertical diffusion. The model was developed to run on a coarse grid. The version used in this study has a horizontal resolution of 8° × 10° (latitude by longitude), and seven layers in the vertical, with a top at 10 mb. This model is called model I (not to be confused with the GISS model developed during the early 1970's). For complete documentation of this model, and an improved version called model II, see Hansen *et al.*, (1983).

Model I was run for five years and the means and standard deviations for each month calculated for a wide variety of diagnostics. Figs. 1a–e show the zonally averaged latitude–height profiles of several quantities at lower latitudes in January (since the Hadley circulation is our main concern we will omit polar regions in this and most other figures). A detailed comparison with observations is given in Hansen *et al.*, (1983). Here it is sufficient to note that the distributions are fairly realistic with the following exceptions [cf. Oort and Rasmussen (1971), Crawford and Sasamori (1981) and Pfeffer (1981)]: 1) the zonal winds increase with height above the observed jet stream level (a function of the location of the model top); 2) the equatorial tropopause temperatures are too warm and polar surface temperatures too cold; 3) eddy kinetic energy is too low at mid- and high latitudes, and 4) the Hadley circulation is about 25% too weak and extends 10–15° too far north. [To make the units in the figures compatible with those in (3), divide (3) by g.] These deficiencies may affect the results of the experiments to be described here; however, when several of the experiments were repeated with the improved model II, the results were of a similar nature. (Due to the nature of some physical process parameterizations, some of the experiments discussed here could not be done with model II.) We may also expect that some of the results will be model dependent; for example, since the model has no explicit diffusion, the momentum budget will probably have a different sensitivity than that of some other GCMs.

Figure 1f shows the standard deviation of the streamfunction for the five January circulations. Each experiment, described here, was run for at least three months starting on 1 December. Although results shown will be for January, no conclusion is drawn if the changes do not also occur in the other winter months. Furthermore, only changes which exceed twice the standard deviations in the control run are considered significant.

To examine the dependence of the Hadley circulation on heat, momentum and moisture forcing, all of which may vary due to climate perturbations, the primary physical processes associated with each of these budgets were removed one at a time, and then in combination (Table 1). The MMC is compared with that of the control run, and its changes are compared to changes in the forcing mechanisms detailed in Eq. (3). However, each change in forcing necessarily produces adjustments in other reactive forcing processes, so we will emphasize the major changes for each experiment with particular attention to these secondary effects where appropriate. Since the model uses specified sea surface temperatures, the full range of feedbacks which might occur in the real atmosphere will not be evident in the model results. For example, if the Hadley circulation increases in intensity, increased surface winds in the model will not result in greater upwelling of equatorial waters and cooler sea surface temperatures [which might provide a negative feedback (e.g., Lau, 1979)]. Also, with only three month integrations, the changes noted are only tendencies and do not necessarily describe equilibrium alterations of the seasonal cycle or the climate.

These experiments are much more extreme than changes which would be encountered in climate perturbations on Earth, though not necessarily more extreme than the variations between Earth and other planetary atmospheres. Their purpose is to highlight the processes that most strongly affect the MMC, reveal the various interactions that occur, and identify which processes must be modeled accurately to obtain proper model sensitivity.

The experiments are divided first into main experiments, whose results are discussed in detail and which involve eliminating specific thermal or momentum forcing processes, and second into associated experiments, which are either combinations of the main experiments or similar to the main experiments except with altered initial conditions.

a. Thermodynamic forcing

Figures 2–6 illustrate the heat and angular momentum budgets in the control run of the model. Figs. 2a–d show that there is a degree of cancellation between heating associated with radiative cooling and moist convective heating at low latitudes, emphasizing the point that the "forcing" for a balanced circulation is not simply related to fixed external parameters but depends also on the circulation. Heating by dry convection and large-scale condensation are only important at lower and upper levels, respectively. Overall, however, $\partial \bar{H}/\partial y < 0$, forcing a direct circulation, but the locations of the heating maxima caused by radiation and convection are influenced by varying solar zenith

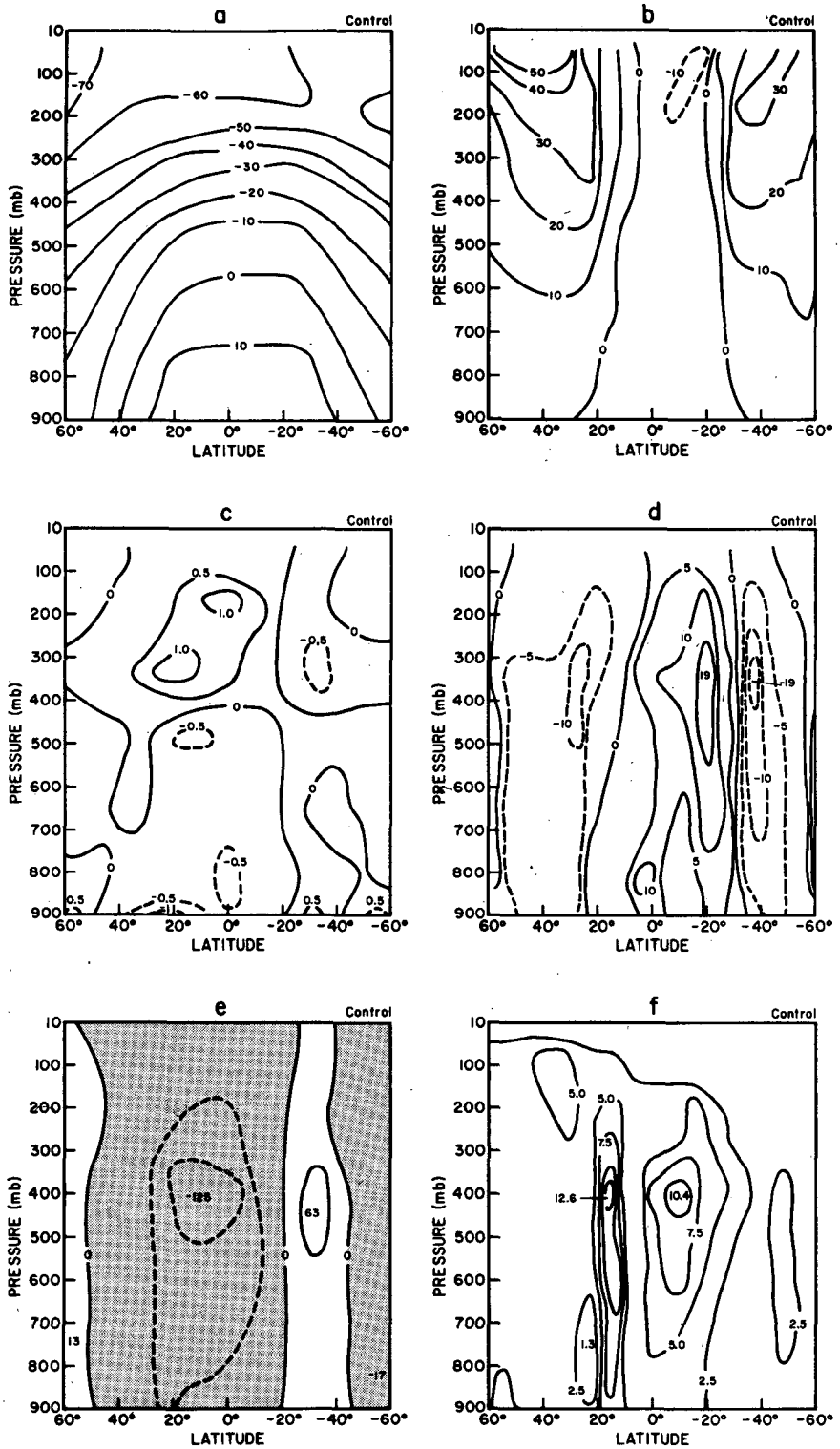

FIG. 1. Zonally averaged latitude-height (pressure) profiles for January for a 5-year run of Model I: (a) temperature (K); (b) zonal wind (m s^{-1}); (c) meridional wind (m s^{-1}); (d) vertical velocity (10^{-5} mb s^{-1}); (e) streamfunction (10^{9} kg s^{-1}); (f) streamfunction standard deviation (10^{9} kg s^{-1}). In these and subsequent figures, dashed lines represent negative values.

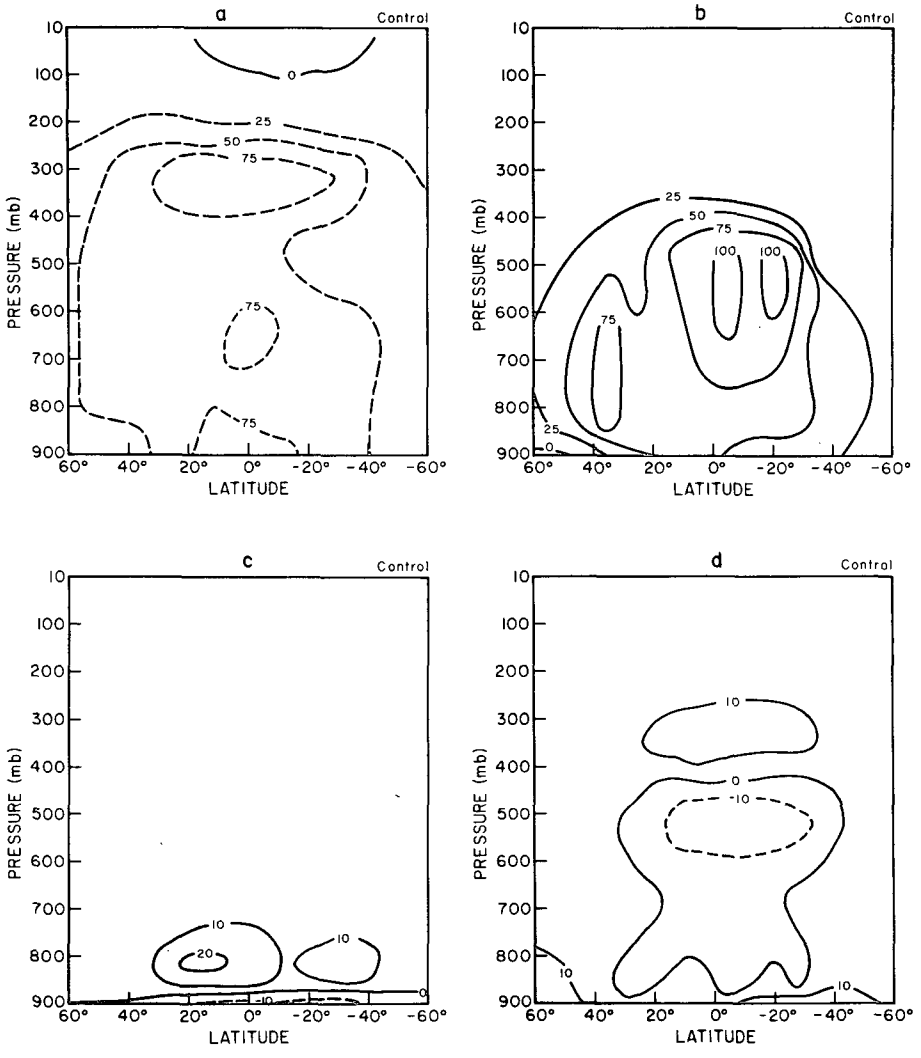

FIG. 2. As in Fig. 1 for the heat budget (10^{13} W): (a) radiational cooling; (b) moist convective heating; (c) dry convective heating; (d) large-scale condensation heating.

angle and sea surface temperature with season, as discussed below.

Figures 3a,b and 4a,b show that most of the low latitude transport of dry static energy (sensible heat plus geopotential energy) is accomplished by the MMC, primarily through the transport of geopotential energy associated with the poleward flow occurring at high altitude. At low levels the heating by MMC vertical heat transport is comparable to that by moist convection. For sensible heat transport alone, the MMC cools the subtropics and heats the tropics, thereby forcing direct circulation in low latitudes; i.e., the heat transport by the MMC reinforces its own amplitude. At higher latitudes eddy transports dominate. The effect of the eddy sensible heat transports is to cool the subtropics and heat higher latitudes thereby driving an indirect (Ferrel) circulation in midlatitudes. These features are in agreement with observations (Oort and Rasmusson, 1971; Vernekar, 1967; Crawford and Sasamori, 1981; Pfeffer, 1981).

The transport of latent heat (moisture) is accomplished about equally by eddies and the mean circulation, except at the lowest levels at low latitudes where the MMC transport predominates (Figs. 3c,d and 4c,d); but vertical transport is also affected by convection as well (not shown). Latent heat transport effects generally reinforce the sensible heat effects thereby intensifying the Hadley circulation (Salustri and Stone, 1983).

The mean circulation is generated in the "dynamics" subroutine in the model, acting on distributions which convection, in the "physics" subroutine, has influenced. This distinction is not made in observational studies, which divide convective fluxes into a zonally averaged part included with mean circulation effects, and a perturbation part included with eddy effects. In fact, the Hadley circulation is occasionally viewed as

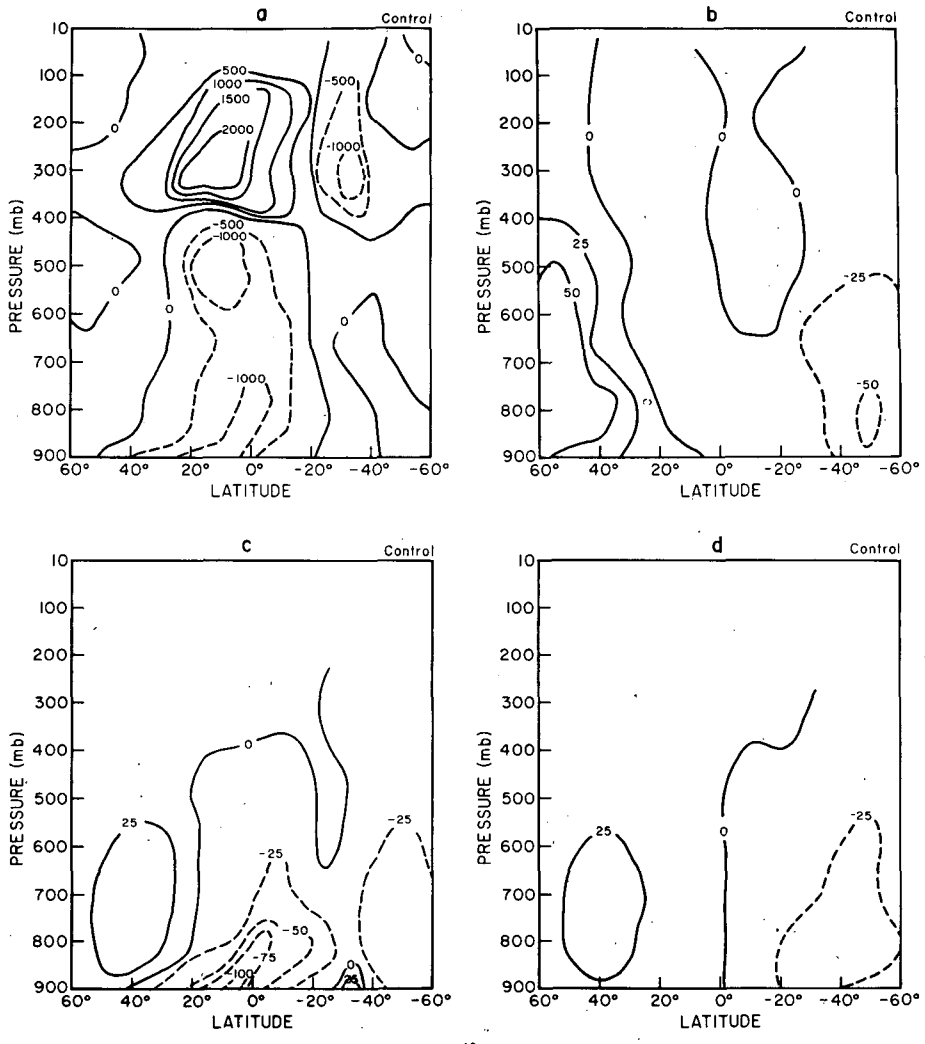

FIG. 3. As in Fig. 1 for northward transports (10^{13} W): (a) dry static energy by the mean circulation plus eddies; (b) dry static energy by eddies; (c) latent heat by the mean circulation plus eddies; (d) latent heat by eddies.

simply the zonally averaged result of individual cumulus "hot towers." We note that this point has not been sufficiently emphasized in comparisons between model results and observations and in discussions of the role of eddies and the MMC. In the model the convection is a subgrid-scale parameterization which is independently monitored, with ascent and compensatory descent within the grid box resulting in no net vertical motion.

The thermal process experiments are as follows.

Exp. 1. The sun is "turned off" so that there is no shortwave radiation. In a specified sea surface temperature model, this means that the only thermodynamic forcing should be the flux of heat (both radiative and sensible) and moisture from the surface which decreases with latitude from a maximum near the equator, as do the sea surface temperatures. (The initial land surface temperatures varied with latitude as well, but they adjust during the integration.)

Exp. 1a. The model is disconnected completely from the radiation routine. No shortwave or longwave radiation occurs.

Exp. 2. The radiation routine is restored, but the sea surface temperature gradient is removed, with all sea surface temperatures set to the global average value of 19°C. This corresponds to the value near 30° latitude, and amounts to a decrease of some 8°C for equatorial waters. Solar radiation is a maximum at subtropical latitudes in the Southern Hemisphere (for December through February), as in the control run.

Exp. 2a. The changes incorporated in runs 1 and 2 are combined, so that there is no gradient in either solar radiation absorption or sea surface temperature. This is an attempt to completely eliminate the latitudinal heating gradients $\partial\bar{H}/\partial y$ associated with the "external" thermodynamic forcing in Eq. (3).

Outside of the changes noted, the physics of the model are unaltered. Convection still mixes momen-

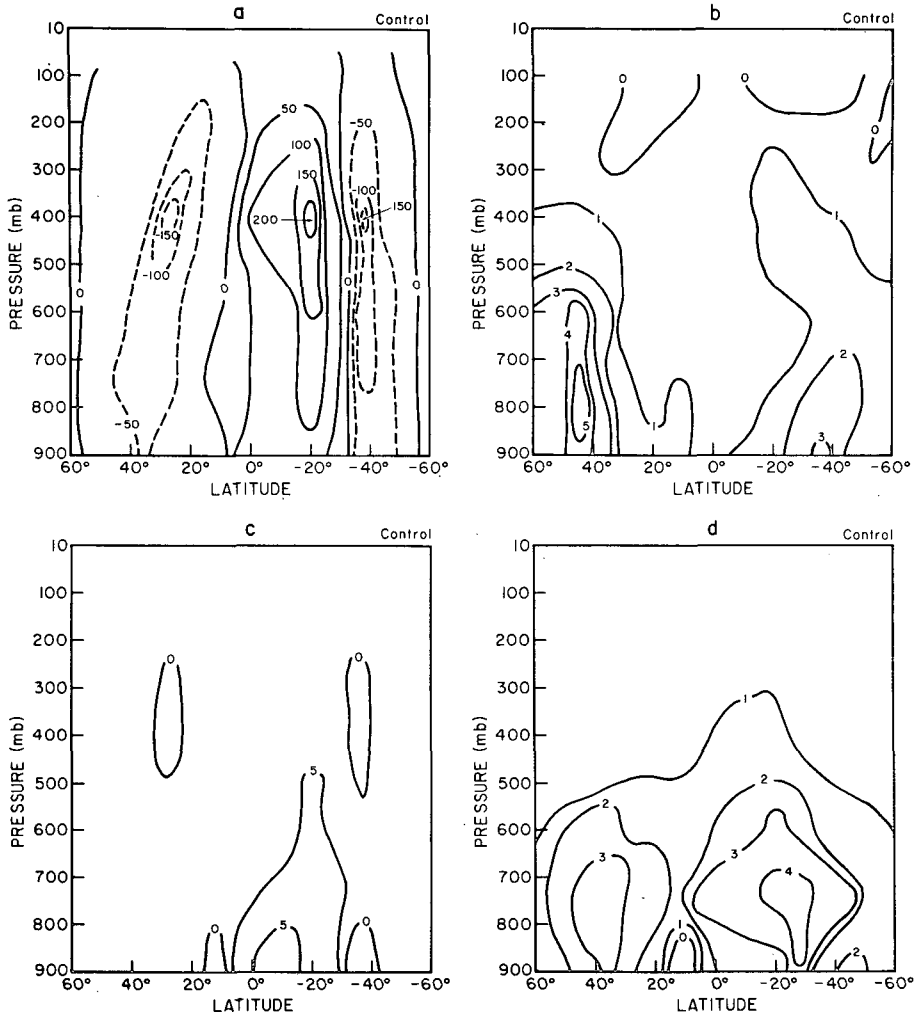

FIG. 4. As in Fig. 1 for vertical transports (10^{14} W): (a) dry static energy by the mean circulation plus eddies; (b) dry static energy by eddies; (c) latent heat by the mean circulation plus eddies; (d) latent heat by eddies.

tum and heat vertically, so that the influence of a low-level heat source is not confined to the lowest levels. Eliminating convection entirely would produce more drastic changes in many model parameters and would obscure the interpretation of the experiments. Similarly, condensation due to large-scale supersaturation still occurs, extending the influence of evaporation to high altitudes. Eliminating condensation would have altered the humidity profile and cloud structure beyond recognition. These comments emphasize the crucial role of various feedbacks in determining a model's response: *feedbacks prevent isolation of a change in external forcing to one aspect of the circulation.* Consequently, study of the MMC response in linearized models misses important responses of the circulation.

b. *Effects of moisture*

In all of the experiments conducted, moisture effects are altered when other forcing terms are changed. However, in the following experiments, the moisture effects are altered directly.

Exp. 3. Evaporation from land and ocean is set to zero. After several months the model is "dry" with no evaporation or condensation. The amount of water vapor in the atmosphere is reduced by 80%. The primary influence of this change is on the thermodynamic forcing, but it cuts across the division made in experiments 1 and 2, and parallels experiments made with other models (e.g., Hunt, 1973).

Exp. 3a. Experiment 3 is repeated with an atmosphere in which the specific humidity is set to zero in the initial conditions and no evaporation is allowed. This model has almost no atmospheric thermal opacity as the primary greenhouse gas has been completely eliminated.

c. *Momentum forcing*

The angular momentum budget is illustrated by the transports shown in Figs. 5 and 6. As shown in Figs.

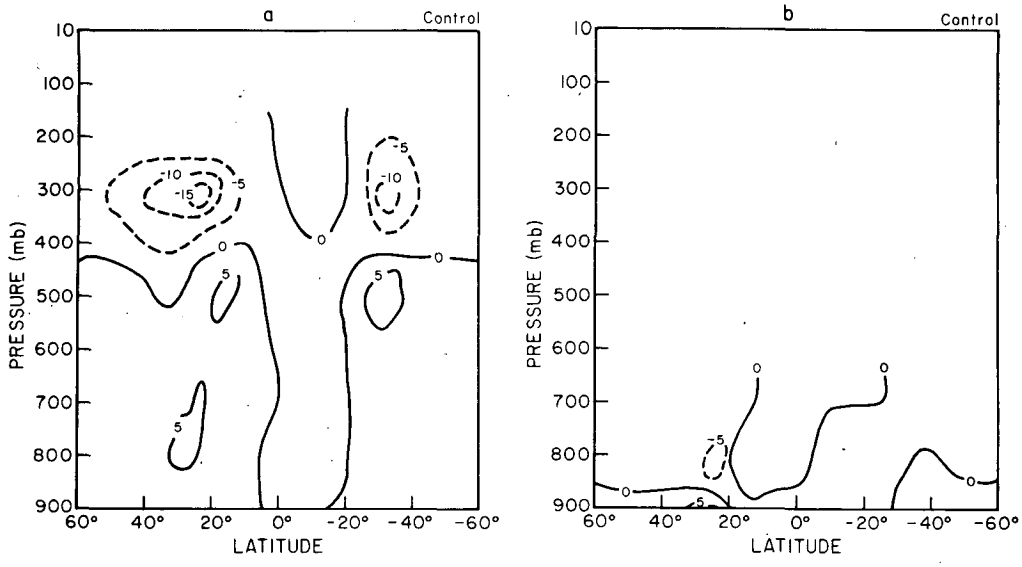

FIG. 5. As in Fig. 1 for change of angular momentum by convection (10^{18} J), in a band of 8° latitude: (a) moist convection; (b) dry convection.

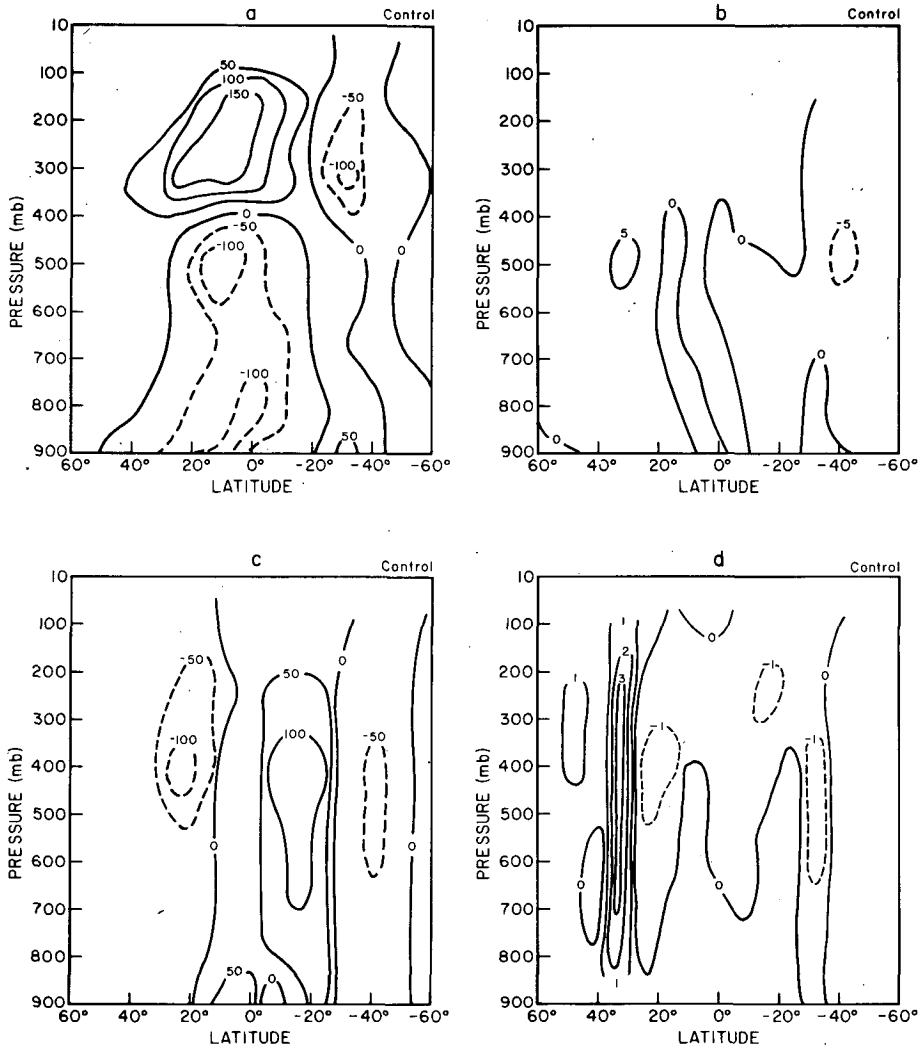

FIG. 6. As in Fig. 1 for transport of momentum (10^{18} J): (a) northward transport by the mean circulation plus eddies; (b) northward transport by eddies; (c) vertical transport by the mean circulation plus eddies; (d) vertical transport by eddies.

5a,b, convection redistributes angular momentum at low latitudes in this model (so-called "cumulus friction"). The vertical distribution is complex but the friction decreases with altitude up to the 400 mb level, forcing a direct circulation in low latitudes. In general, however, vertical transport of angular momentum at low latitudes is dominated by the MMC, with westerly momentum lifted out of the lowest layers and transported poleward at high altitudes (Figs. 6a,c). This transport of *angular* momentum represents a deceleration of $\bar{u}$, because $\partial\bar{u}/\partial y$ and $\bar{v}$ are positive and $(\partial/\partial p)(\bar{v}\partial\bar{u}/\partial y) < 0$ in Eq. (3); hence this transport by the MMC strengthens direct circulation. The eddy contribution becomes significant at midlatitudes where it generates an indirect circulation. These features are in general agreement with observations (Oort and Rasmussen, 1971; Vernekar, 1967; Crawford and Sasamori, 1981; Pfeffer, 1981).

Each of the friction processes is eliminated one by one in the following experiments to judge their individual effect, and then together to gauge the importance of momentum forcing in general.

Exp. 4. The surface stress source of momentum is eliminated by setting the drag coefficient to zero; however, the surface sensible and latent heat fluxes are retained.

Exp. 5. The surface stress is only one component of the surface influence on momentum; mountain drag, due to the variation of pressure from the windward to leeward sides of mountains, may be of comparable magnitude. Thus, both the topography and the surface drag coefficient for momentum are set to zero in this experiment. This eliminates the surface as a direct momentum forcing mechanism.

Exp. 5a. Experiment 5 is repeated with initial conditions which have no winds, i.e., the relative angular momentum is zero everywhere. This is to determine whether the effect on the mean circulation is dependent upon the (initial) amount of angular momentum (which remains unchanged with no surface stress).

Exp. 6. Since there is no explicit diffusion in the model, the only other friction enters in the convective parameterization. The momentum mixing by both dry and moist convection is set to zero; the surface friction effects, due to both drag and topography, are restored.

Exp. 6a. Momentum forcing is completely eliminated by combining experiments 5 and 6. With no surface friction, topography, or momentum mixing by convection, the only generating processes for the mean circulation are thermodynamic forcing and eddy heat and momentum convergences.

A complete list of the experiments is shown in Table 1. In summary, in this set of experiments we alter the main boundary forcings (radiation, sensible and latent heat fluxes, surface friction and topography) and the mechanisms which transmit the forcing into the interior of the atmosphere (momentum mixing by convection and latent heat release). Some of these processes could be considered as localized forcing, associated with particular climate zones, but the feedbacks of the altered MMC and large-scale eddy processes link the climate zones together. This is especially true when moisture effects are considered. Fig. 7 shows the distribution of $\partial\bar{G}/\partial y$ and $f\partial\bar{L}/\partial p$ in the model: the two eddy effects are comparable at subtropical latitudes and midlatitudes as observed (cf. Crawford and Sasamori, 1981; Pfeffer, 1981). As we illustrate, eddy motions and the hydrological cycle provide many different alternative adjustments of the MMC to its external constraints. This complexity accounts for the difficulty in determining the sensitivity of the MMC to changed forcing.

TABLE 1. Description of experiments.

Experiment	Description
1	No solar radiation
2	Uniform sea surface temperatures (19°C)
3	No evaporation
4	No surface friction
5	No surface friction and no topography
6	No momentum mixing by convection
Associated experiment	**Description**
1a	No radiation, solar or terrestrial
2a	No solar radiation, uniform sea surface temperatures (19°C)
3a	No evaporation, zero specific humidity
5a	No surface friction, no topography, zero initial winds
6a	No surface friction or topography, no momentum mixing by convection

4. Results

In this section we describe the results of the individual experiments, while in Section 5 we discuss the effect on specific Hadley cell characteristics.

a. Experiment 1

In this experiment solar radiation is eliminated. With climatologically specified sea surface temperatures, the ocean becomes the primary heat source for the model. Although initially acting as a low-level source, heat (sensible and latent) from the ocean surface is quickly mixed vertically by moist convection in such a way as to minimize the temperature changes in the model. Zonally averaged land surface temperatures are 5°C cooler at low latitudes, 5–10°C cooler at subtropical latitudes, and slightly warmer at high latitudes, due to increased eddy transports, as discussed below.

The January Hadley circulation resulting from this experiment is shown in Fig. 8. Compared with the year-to-year variation in the streamfunction for January (Fig. 1f), the changes shown in Fig. 8 are generally ten times the standard deviation, and thus highly significant. (This will be true for all the experiments, so

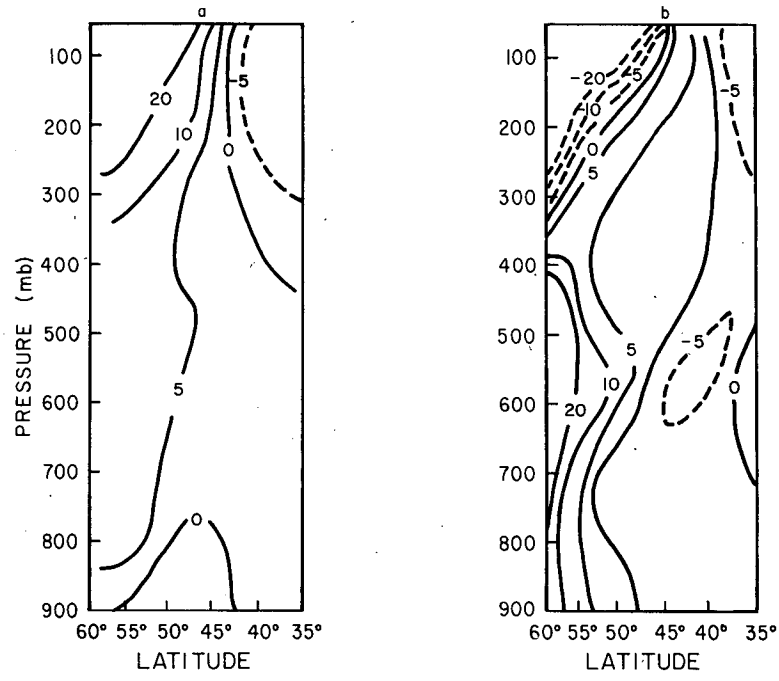

FIG. 7. Forcing of the mean circulation at midlatitudes in January in Model I by: (a) change with latitude of eddy heat flux convergence; (b) change with altitude of eddy momentum flux convergence. Units are m^2 (kg s)$^{-1}$. Positive values indicates Ferrel cell generation.

this comment will not be repeated.) The most obvious changes are the intensification and narrowing of the Northern Hemisphere (hereafter referred to as NH) Hadley cell, with the peak shifted 8° to the north, and the establishment of a Southern Hemisphere Hadley circulation beginning at the equator. These changes can be related directly to the changed thermal forcing. In the control run maximum solar radiation in January is absorbed in the Southern Hemisphere (SH) as shown in Fig. 9. (This picture remains relatively constant in the experiments, except for 1 and 1a.) Latent heat release by condensation is a maximum at about 20°S in the control run, as can be seen from Figs. 2b,d, and also Fig. 10a, which gives the variation of precipitation with latitude. Fig. 10b shows the evaporation as a function of latitude. The slight maximum in the control run evaporation in the region where solar radiation absorption is maximum combines with moisture convergence by the dynamics to produce the local rainfall maximum. In experiment 1 (Fig. 10b), removal of solar radiation forcing of surface energy fluxes shifts the evaporation maximum to the equator, coincident with the location of the sea–surface temperature maximum in January. Thus, the rainfall maximum also shifts toward the equator. This distribution of latent heating provides the thermal forcing for Hadley circulations in both hemispheres.

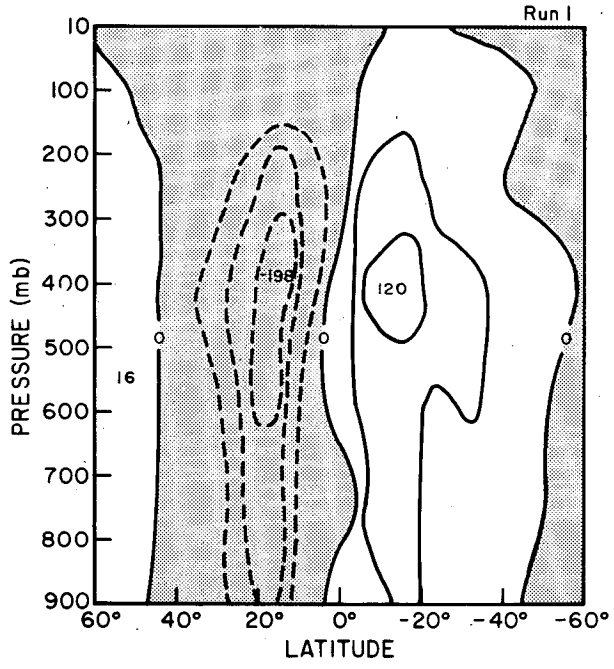

FIG. 8. January streamfunction for experiment 1 (10^9 kg s^{-1}). In this and subsequent streamfunction depictions negative values of the streamfunction are indicated by dashed contours and shading.

There are several positive feedbacks involved in these adjustments. As the Hadley circulation intensifies in a certain area, larger surface winds increase the evaporation and moisture available for condensation. As precipitation begins, latent heat release destabilizes the atmosphere (in a CISK-type feedback) reinforcing updrafts. Consequently, increased precipitation is associated with increased intensity of the Hadley circulation

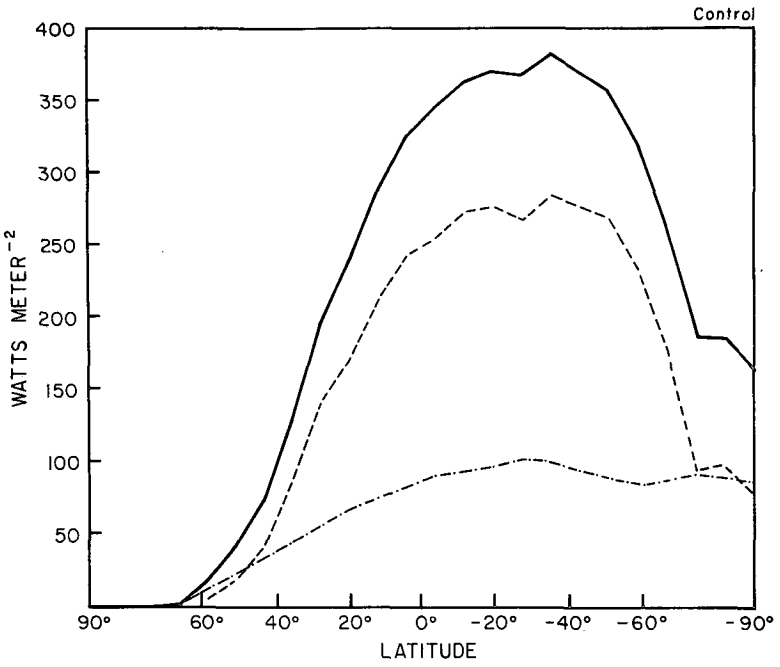

FIG. 9. Absorbed solar radiation in the control run in January as a function of latitude at the ground (dashed line), in the atmosphere (dot-dashed line), and the sum (solid line).

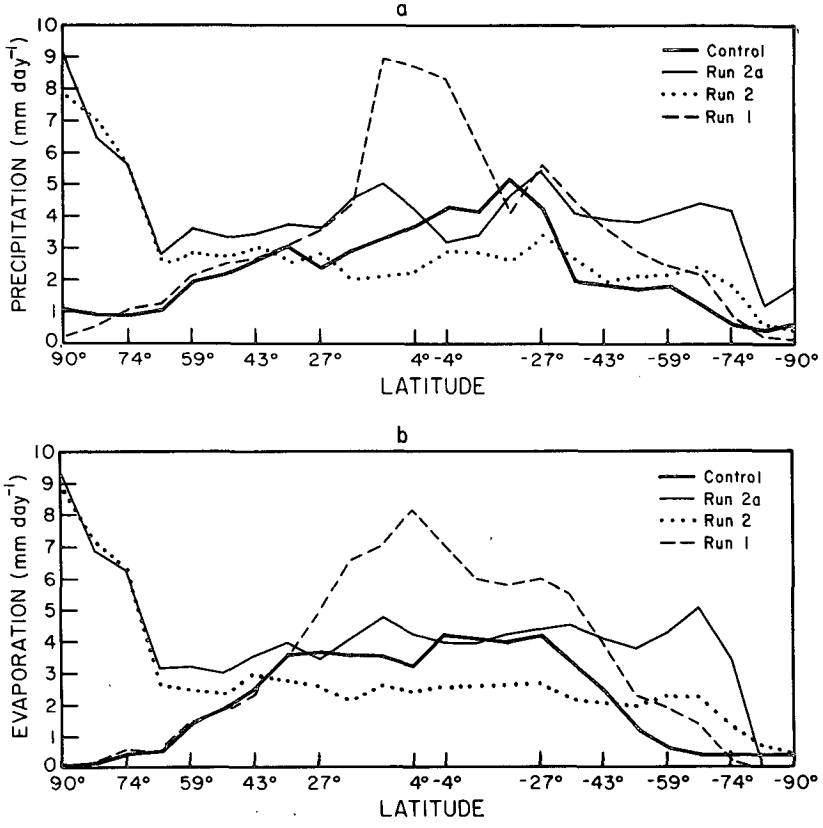

FIG. 10. (a) Precipitation and (b) evaporation as a function of latitude during January in the control run and in experiments 1, 2 and 2a.

TABLE 2a. Momentum balance as a function of latitude at 937 mb in the control run. Column headings refer to the terms in Eq. (6). All quantities are in units of 10^{-5} m s^{-2}.

Latitude	$f\bar{v}$	Δ_HE	Δ_HMC	Δ_VE	Δ_VMC	D_{DC}	D_{MC}	D_{SF}	D_{MD}
59°		0.0	0.3						
55°	6.6			−0.0	0.6	0.2	0.1	−1.2	−0.1
51°		−0.0	−3.4						
47°	−4.1			−0.0	2.0	0.2	0.2	−0.8	0.3
43°		0.1	−2.2						
39°	−7.7			−0.0	2.5	0.2	0.4	−0.6	0.3
35°		−0.1	−1.6						
31°	−9.0			−0.1	2.2	0.3	0.2	−0.1	0.2
27°		0.2	−2.2						
23°	−8.5			−0.0	0.8	0.4	0.1	0.2	0.2
20°		0.0	−2.0						
16°	−4.4			−0.0	−0.3	−0.1	0.0	0.5	0.1
12°		−0.0	0.1						
8°	−2.1			−0.0	−2.8	−0.1	0.0	0.3	0.0
4°		−0.0	4.4						
0°	0			−0.0	−2.4	0.0	0.0	0.1	−0.0
−4°		0.0	0.4						
−8°	0.3			−0.0	0.1	0.0	0.0	−0.0	−0.1
12°		−0.0	0.5						
−16°	0.2			−0.0	−2.0	0.0	0.1	−0.0	−0.2
−20°		−0.0	2.5						
−23°	−2.7			−0.0	−3.1	0.0	0.1	0.4	−0.2
−27°		0.0	1.9						
−31°	−7.3			−0.0	0.8	0.2	0.2	0.5	−0.2
−35°		−0.0	−2.8						
−39°	−3.1			−0.0	3.0	0.2	0.2	0.0	−0.1
−43°		−0.0	−2.0						
−47°	2.1			−0.0	1.8	0.1	0.1	−0.4	−0.0
−51°		−0.0	−1.0						
−55°	7.0			−0.0	−0.2	0.0	0.0	−0.9	−0.0
−59°		−0.0	1.3						

updrafts; in other words, the thermal forcing can also be looked upon as a response to other forcing changes as well as being a cause for circulation changes. The thermal forcing term in Eq. (3), $\partial\bar{H}/\partial y$, changes because increased precipitation at low latitudes increases the latitudinal gradient of condensational heat release (Fig. 10a).

In steady state the angular momentum balance for a vanishingly thin annulus of the atmosphere can be written as

$$f\bar{v} = \frac{\partial}{\partial y}(\overline{v'u'}) + \frac{\partial}{\partial y}(\bar{v}\bar{u}) + \frac{\partial}{\partial p}(\overline{\omega'u'}) + \frac{\partial}{\partial p}(\bar{\omega}\bar{u}) + D_{DC} + D_{MC} + D_{SF} + D_{MD}. \quad (6)$$

The first two terms on the right (Δ_HE and Δ_HMC) are the horizontal divergences of momentum by eddies and the mean circulation, respectively, while the next two terms (Δ_VE and Δ_VMC are the vertical divergences by eddies and the mean circulation. The last four terms represent the divergence of momentum by dry convection, moist convection, surface friction and mountain drag. Table 2a illustrates the balance in the control run at 937 mb and Table 2b the balance at 315 mb. (Note that *convergence* is shown in the table. Due to the staggered grid representation, the horizontal convergences are actually calculated at the edges of the grid box, so exact balance cannot be shown; furthermore, numerical resolution is insufficient in some cases.) Table 2 shows that the predominant terms producing MMC momentum ($f\bar{v}$) are the convergences associated with the MMC itself, but that the MMC horizontal and vertical convergences largely offset one another. Consequently, all of the smaller contributions from the other terms can be important: the eddy contribution is minimal at both levels at low latitudes; surface effects are important only at the lowest level; and moist convection is more important at higher levels.

This balance implies that when altered thermal forcing initiates a change in the Hadley circulation, momentum balance can be restored by further changes in the MMC to effect a compromise between thermal and momentum requirements. This is illustrated by the changes in the angular momentum balance and the mean meridional velocity for experiment 1 shown in Fig. 11a for 937 mb, and in Fig. 11b for 315 mb. The wind change is effected largely by offsetting changes in the vertical and horizontal convergence of angular momentum by the MMC, while the direct eddy contribution is negligible. This alteration of momentum transfer by both the vertical and horizontal components of the mean circulation, itself, prevents the determination of the $\bar{v}$ wind from the stresses alone [in Eq. (1), omitting the nonlinear terms], as would be the case in a simple quasi-geostrophic system.

TABLE 2b. As in Table 2a except at 315 mb.

Latitude	$f\bar{v}$	$\Delta_{//}E$	$\Delta_{//}MC$	$\Delta_{\nu}E$	$\Delta_{\nu}MC$	D_{DC}	D_{MC}
59°		0.4	0.6				
55°	0.4			0.0	−1.2	0.0	−0.5
51°		0.0	1.5				
47°	2.7			0.0	−1.9	0.0	−0.7
43°		−0.1	1.5				
39°	3.9			−0.1	−1.5	0.0	−0.8
35°		−0.1	1.0				
31°	4.0			0.0	−2.8	0.0	−0.6
27°		−0.5	5.5				
23°	6.0			−0.1	−2.8	0.0	−0.9
20°		−0.2	−0.5				
16°	4.2			−0.0	0	0.0	−0.4
12°		0.2	−0.4				
8°	1.2			0.1	1.8	0.0	−0.2
4°		−0.1	−3.4				
0°	0			0.0	2.7	0.0	0.0
−4°		0.0	−2.3				
−8°	−0.8			0.0	2.0	0.0	0.0
−12°		−0.0	−2.0				
−16°	−0.6			0.0	3.3	0.0	0.0
−20°		0.1	−3.9				
−23°	1.9			0.0	3.7	0.0	−0.2
−27°		−0.5	−3.2				
−31°	5.5			−0.1	−0.8	0.0	−0.6
−35°		−0.3	4.1				
−39°	2.3			−0.0	−2.5	0.0	−0.2
−43°		0.0	1.1				
−47°	1.2			0.0	−0.7	0.0	−0.4
−51°		0.3	0.3				
−55°	0.6			0.0	0.0	0.0	−0.5
−59°		0.8	−0.1				

The direction and intensity of the meridional wind is closely correlated with the distribution of all the other friction processes in a fashion similar to the directly associated surface friction. This suggests an important role for these other processes in determining how the MMC will adjust as is more clearly displayed in Table 3, which shows the meridional winds at the lowest model level, along with the surface friction, pressure gradient (mountain drag) and convective mixing (cumulus friction) changes of angular momentum for that level at various latitudes. (The mountain drag effect is not actually restricted to the 937 mb level, as mountains extend above that, but it is limited to the first sigma level which has a mean pressure of 937 mb.) If friction is thought of as an "external" forcing for the MMC, then from Eq. (6) the meridional wind must be equatorward when angular momentum is being added to the atmosphere, in order to effect a balance with the Coriolis force. Because friction is actually a "reactive" force, the sense of this relationship is maintained despite the dominance of the MMC advection terms in Table 2: in the Northern Hemisphere the winds are northerly where friction effects add momentum and southerly where angular momentum is being removed. In run 1, where the low-level meridional wind switches direction at low southern latitudes, the total frictional forcing also changes sign. Figs. 11a,b confirm that relatively small changes in surface effects and convection in all the experiments are always consistent with the sense of the circulation. Where angular momentum is increased by these processes, relative to the control run, the winds become more equatorward, moving air so as to increase its distance from the earth's axis. Thus friction terms give the sense of the acceleration of the MMC by the surface, but once in motion the strength of the MMC is amplified or diminished by its own momentum advection. In other words, the adjustment of the MMC to altered forcing involves both the changes in MMC transports and these other reactive stresses, not simply in one or the other alone.

The changes in experiment 1 shown in Table 3 also illustrate other important adjustments. Since convection is a key participant in the near-surface friction adjustments and the only friction process at high levels, changes in thermal forcing also affect the angular momentum balance in the model by influencing convec-

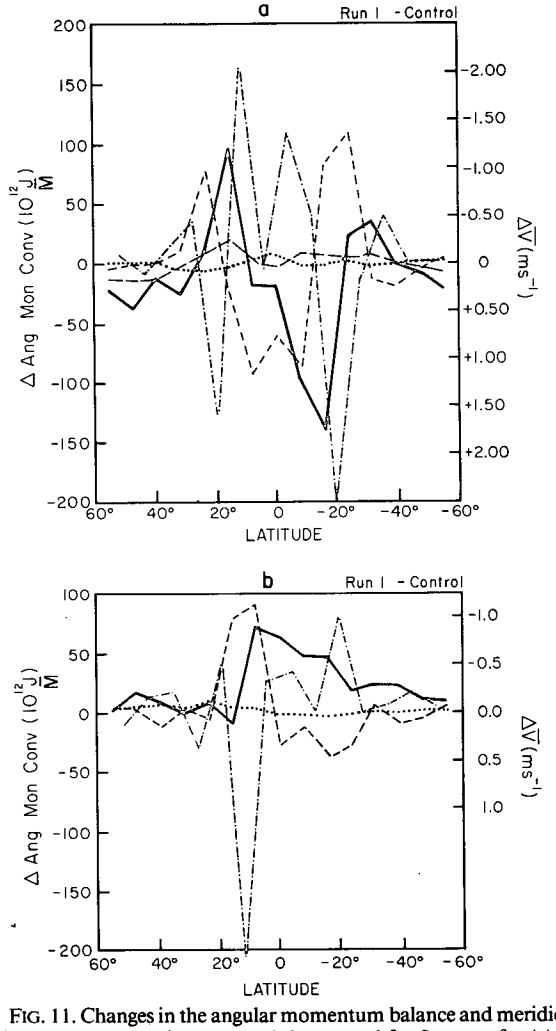

FIG. 11. Changes in the angular momentum balance and meridional wind between experiment 1 and the control for January for (a) 937 mb and (b) 315 mb. Shown is the change in horizontal convergence of angular momentum (dot-dashed), change in vertical convergence (dashed), convection effect (dotted), surface effect at 937 mb (long dashes), and meridional wind change (solid line).

TABLE 3a. Meridional wind (10^{-2} m s^{-1}) and change of angular momentum (10^{-4} J m^{-3}) by different drag mechanisms as a function of latitude for the control run and experiments 1–3. (SF = surface friction; MD = mountain drag.)

	Control run					Experiment 1				
Latitude	$\bar{v}$	SF	MD	Convection	Total	$\bar{v}$	SF	MD	Convection	Total
55°	56	−39	−172	701	−3374	52	−5855	869	1402	−3584
47°	−39	−3117	1113	1776	−228	2	−5132	979	2157	−1996
39°	−84	−2876	1177	2568	869	−47	−3839	1038	2903	102
31°	−120	−438	1181	3008	3751	−69	−226	1146	1149	2069
23°	−150	962	1098	2927	4987	−138	3148	873	913	4934
16°	−109	2842	351	−899	3103	−232	6300	217	−90	6427
8°	−103	2102	134	−699	1537	−68	1184	96	408	1688
0°	−21	540	−52	−462	26	7	−764	−70	1443	609
−8°	−14	−3	−467	175	−295	85	2081	166	−175	2072
−16°	−6	−83	−1068	420	−731	139	2872	662	300	3834
−23°	48	2224	−1233	283	1274	31	−89	385	692	988
−31°	97	2934	−880	1960	4014	63	1369	335	108	2785
−39°	34	166	−354	1786	1598	39	209	202	1489	1900
−47°	20	−1823	−142	719	1246	−8	−1581	40	931	−610
−55°	−59	−3608	−68	350	−3326	−34	−3088	31	901	−2156

tion. Note further that the changed surface effect is shared by both the surface friction and the mountain drag; thus, realistic topography is required to ascertain the surface effects properly.

While the eddy transport of angular momentum at low latitudes does not appear to provide significant forcing of the MMC, the eddies can still influence the Hadley circulation by transporting heat. Rewriting (2) in terms of temperature explicitly, we have

$$\frac{\partial \bar{T}}{\partial t} + \bar{v}\frac{\partial \bar{T}}{\partial y} + \bar{\omega}\left(\frac{\partial \bar{\theta}}{\partial p}\right) = \bar{H} - \frac{\partial}{\partial y}(\overline{v'T'}) - \frac{\partial}{\partial p}(\overline{\omega'T'}). \quad (7)$$

In the lower stratosphere, the first and second terms on the left and the last term on the right are generally assumed to be small, at least under certain conditions (e.g., Dunkerton, 1978). The two remaining terms on the right are the horizontal convergence of sensible heat flux by eddies and the heating (purely radiative in the stable stratosphere). Each effect generates a mean vertical velocity $\bar{\omega}$—in other words, a mean circulation. To isolate the circulation driven by heating, we can define a "transformed" vertical velocity $\bar{\omega}^*$ (e.g., Dunkerton, 1978) as

$$\bar{\omega}^* \equiv \bar{\omega} - \frac{\partial}{\partial y}\left[(\overline{v'T'})\left(\frac{\partial \bar{\theta}}{\partial p}\right)^{-1}\right], \quad (8)$$

and similarly a transformed meridional velocity $\bar{v}^*$ and a transformed streamfunction $\bar{\psi}^*$,

$$\bar{v}^* \equiv \bar{v} - \frac{\partial}{\partial p}\left[(\overline{v'T'})\left(\frac{\partial \bar{\theta}}{\partial p}\right)^{-1}\right],$$

$$\frac{\partial \bar{\psi}^*}{\partial y} = \bar{\omega}^*, \quad \frac{\partial \bar{\psi}^*}{\partial p} = -\bar{v}^*. \quad (9)$$

The mean circulation induced by the eddy heat transport is thus excluded from the transformed streamfunction which is generated only by direct heating ($\bar{H}$).

In the tropical troposphere the balance is quite different. The dominant terms in (7) are heating by moist convection and cooling by radiation, as can be seen in Figs. 2–4. However, both of these processes appear as subdivisions of total $\bar{H}$ in our notation. The second and third terms on the left are the transport of heat by the MMC, which will react to changes initiated by other forcing terms in much the way the transport of angular momentum by the MMC reacts. At the lowest latitudes, the third term on the right becomes small, and during January the temperature change with time is small at low latitudes. All of these factors allow us to use the concept of the transformed streamfunction to illustrate the qualitative effect of heating changes where they predominate; the transport of heat by the mean circulation will amplify or diminish the streamfunction.

Here we define the eddy effect as due only to the convergence of eddy sensible heat transport, even though eddies also transport latent heat (Salustri and Stone, 1983). They may also establish a moist static energy profile conducive to moist convective heat release. Nevertheless, we will discuss the eddy-induced mean circulation without reference to latent heat.

At higher latitudes, eddy momentum transports must also be considered. They alter the mean wind shear, and thus, from the thermal wind relationship, the temperatures and temperature gradient by inducing adiabatic vertical motions. Thus eddy momentum effects also enter the equations through the temperature, stability or infrared cooling terms. This effect cannot be represented by the transformed streamfunction analysis, but will be discussed separately.

Figure 12a shows how the transformed streamfunction changes in experiment 1 relative to the control run. The changes in the heating are associated with increased condensation centered at 12°N (Fig. 10a) and removal of the shortwave absorption gradient at higher latitudes (Fig. 9). These effects are apparent in Fig. 12a as circulations spiral away from 12°N and

TABLE 3a. (*Continued*)

Experiment 2					Experiment 3				
$\bar{v}$	SF	MD	Convection	Total	$\bar{v}$	SF	MD	Convection	Total
−17	−948	1637	−100	589	−35	−2255	1212	2103	1060
−16	−3206	2462	677	−67	−114	−2306	2077	4272	4043
−32	−2619	2200	521	102	−118	−2866	2959	4131	4224
−45	−1603	2043	1419	1859	−128	−3572	2849	6073	5360
−23	−1414	1450	1102	1138	−111	−984	1275	3431	3722
−25	365	473	−300	538	−118	2509	383	390	3282
−111	1648	374	−291	1731	−109	3164	247	−1749	1662
−72	535	134	−375	294	−85	959	−62	−751	146
−22	−563	−101	321	−343	−28	−726	−925	729	−922
−19	16	−640	−420	−1044	−35	378	−2537	−456	−2609
1	−903	−542	818	−627	48	3352	−2827	346	871
−16	−647	−344	304	−687	75	1564	−1641	3481	3404
16	267	−221	633	679	31	−896	−650	3089	1543
−4	−439	73	127	−239	6	−1065	−214	1734	455
−2	−203	−4	100	−107	11	−307	−66	951	57

weaker gradients at higher latitudes generate more indirect circulation in both hemispheres.

Figure 12b shows the difference between the change in total streamfunction (Fig. 8 minus Fig. 1e) and the change in transformed streamfunction (Fig. 12a), or, in other words, estimates of the alterations produced by the changed eddy heat flux convergence. Although fixed sea surface temperatures keep atmospheric temperatures above the oceans to within 5–10°C of those in the control run, temperatures over land fall by up to 30°C at low levels in low latitudes. This creates a strong increase in (standing) eddy available potential energy, and nearly doubles eddy kinetic energy. Eddy transports increase by a similar factor, actually helping to warm high latitudes slightly. Where the change in eddy heat transports produces stronger maxima, an indirect circulation develops (Fig. 12b, e.g., at 31°N) and where it produces stronger minima (e.g., 16°N) a stronger direct circulation is forced. This effect is in addition to the circulation generated by the new heating distribution. A comparison between Figs. 8, 12a and 12b shows that the sense of the changed circulation is that produced primarily by the changes in thermal forcing, but the eddy contributions are not negligible. Thus, some of the adjustment in the angular momentum balance through altered transport by the MMC is necessitated by the additional changes in eddy heat transport.

This experiment indicates that a coherent, sharply peaked heat source in the model can generate a stronger Hadley circulation than that produced by the normally diffuse heat source, which consists of the combined effects of radiation absorption plus latent heat release (cf. Schneider and Lindzen, 1977). The angular momentum balance is achieved largely through altered momentum transport by the MMC, itself, effecting a compromise between changes in the friction processes and changes in eddy heat transports. All of these

TABLE 3b. Meridional wind (10^{-2} m s^{-1}) and change of angular momentum (10^{-4} J m^{-3}) by the different drag mechanisms as a function of latitude for experiments 4–6.

	Experiment 4				Experiment 5		Experiment 6				Experiment 6a
Latitude	$\bar{v}$	Convection	MD	Total	$\bar{v}$	Convection	$\bar{v}$	SF	MD	Total	$\bar{v}$
55°	64	300	−4243	−3943	−4	250	45	−3092	156	−2936	6
47°	67	465	−4305	−3840	−13	550	2	−3032	947	−2085	−3
39°	−13	1191	−1757	−566	−15	856	−53	−1000	526	−474	−3
31°	−94	2028	1514	3542	−31	1250	−71	862	800	1662	0
23°	−112	2518	1173	3691	−83	2203	−62	893	796	1689	−8
16°	−76	1349	494	1843	−106	2249	−113	2863	405	3268	−6
8°	−81	1195	236	1431	−97	1661	−146	1681	353	2034	−43
0°	−8	289	1	290	−14	462	−51	−453	69	−384	−143
−8°	3	58	98	156	−23	−29	5	467	−254	−213	−54
−16°	39	150	655	805	9	300	−51	−1044	−883	−1927	−18
−23°	71	1039	1079	2118	49	1605	57	3034	−1513	1521	−4
−31°	46	1250	215	1465	48	1690	52	3159	−1066	2093	4
−39°	20	1116	−401	715	28	1228	8	613	−318	295	8
−47°	5	508	−116	392	11	592	−29	−1671	−171	−1842	1
−55°	−3	51	−79	−28	1	76	−47	−2622	−40	−2662	−4

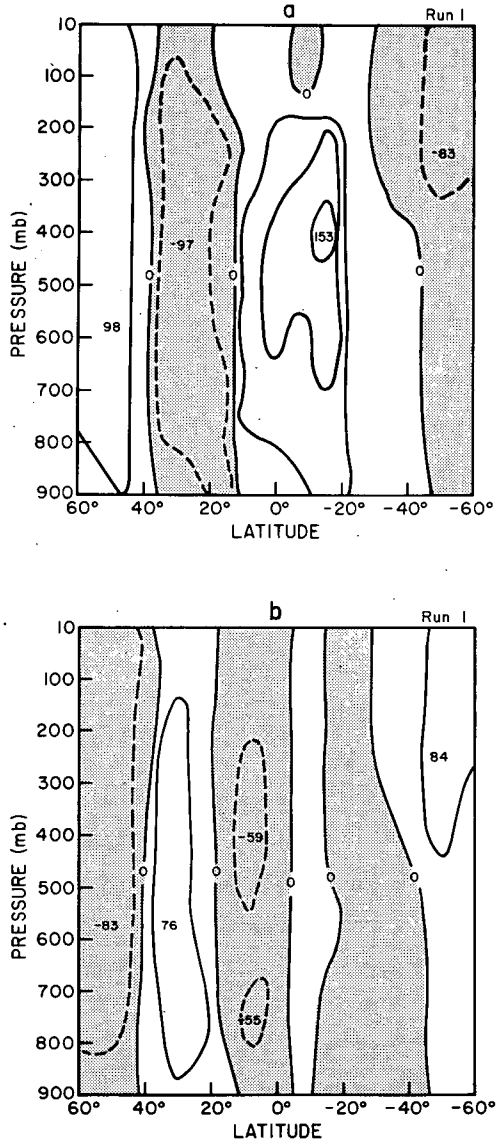

FIG. 12. Change in (a) the transformed streamfunction and (b) in the eddy heat flux induced circulation between run 1 and the control (10^9 kg s^{-1}). (See text.)

changes are also coupled through the altered hydrological cycle.

b. Experiment 2

The latitudinal gradient in sea surface temperature is removed. As noted in Section 3, the specified sea surface temperature of 19°C is consequently 8°C cooler near the equator than in the control run. Low latitudes cool by that amount; at high latitudes temperatures increase by up to 18°C, commensurate with the increased sea-surface temperatures in those regions. Evaporation and precipitation no longer show a low-latitude maximum (Figs. 10a, 10b). The resultant mean circulation is shown in Fig. 13a. The circulation is weakened somewhat, and shifted southward in the

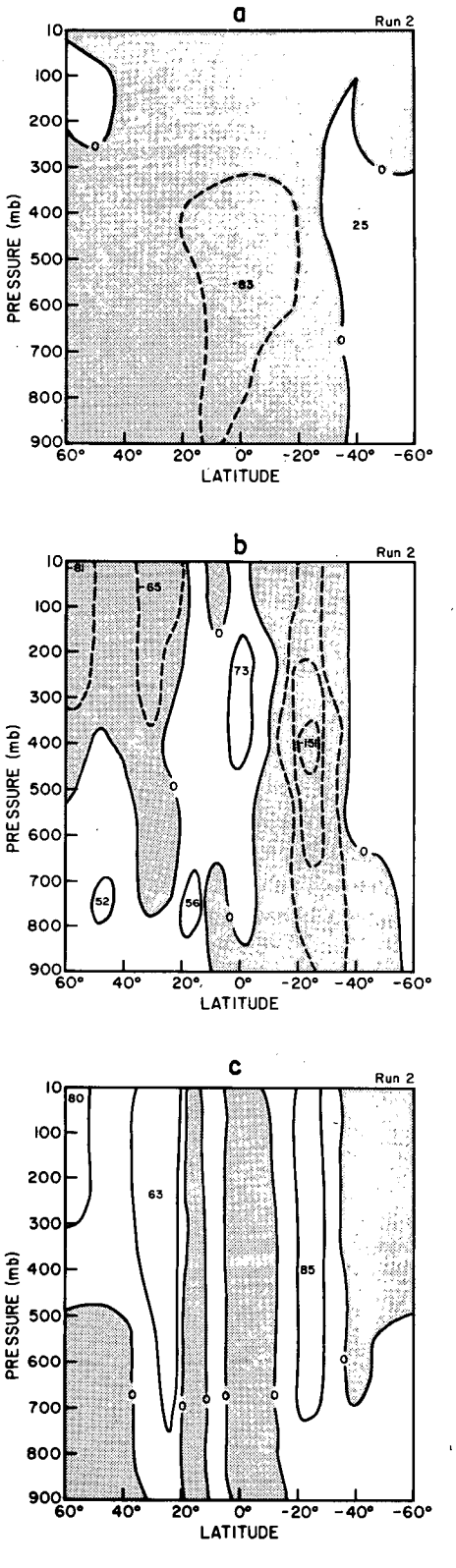

FIG. 13. (a) Streamfunction for experiment 2; (b) changes between run 2 and the control for the transformed streamfunction; and (c) change in the eddy heat flux induced circulation.

Southern Hemisphere. This situation is the reverse of the previous one: by eliminating the influence of the latitudinal sea surface temperature gradient on latent heat release, the radiation absorption gradient becomes predominant. Rising air is now concentrated at 35°S, where the radiation absorption is a maximum (Fig. 9), and both the Hadley cell to the north and a reverse circulation to the south begin and are amplified there. However, as Fig. 10 shows, there is no significant peak in precipitation at this latitude, suggesting that surface sensible and latent heat fluxes play more of a role in determining the location of this feature. The Northern Hemisphere part of this circulation is substantially weakened, because the magnitude of $\partial\bar{H}/\partial y$ is reduced with the more uniform distribution of latent heating.

At most latitudes, the angular momentum balance is maintained by changes in momentum transport by the MMC as in experiment 1. In Table 3a the circulation changes produce reactive changes in the frictional forcing, in the sense that the equatorward wind decreases where angular momentum deposition by the drag processes decreases in the lowest layer. The details of the changes in the frictional drag terms show complicated partitioning among the surface drag, mountain drag and cumulus friction.

The eddy kinetic energy in this experiment is reduced by about a factor of 2 by increased sea surface temperatures at high latitudes. This reduces eddy transports (and MMC transports as well) of heat and angular momentum to negligible values throughout midlatitudes, while at low latitudes transports are reduced by 2–3 times. North of 55°N a change of the vertical gradient of eddy convergence of angular momentum, associated with the reduction in eddy transports aloft, helps generate an increased direct circulation.

Figure 13b shows the change in the transformed streamfunction. The thermally driven circulations in the Southern Hemisphere and the weakening of the one in the Northern Hemisphere appear clearly. Fig. 13c shows the effect of the changed eddy heat transports on the meridional circulation. Near the equator the changes are small, in contrast to experiment 1 in which eddy energy at low latitudes changed strongly. In the Southern Hemisphere subtropics, decreased heat transport by eddies weakens the indirect circulation. In the Northern Hemisphere, eddy heat transports now converge at lower midlatitudes as eddy energy decreases further north and the influence of the warm sea surface temperatures actually produces negative heat transports in the lowest levels at upper midlatitudes. This results in changed eddy induced circulations spiraling away from midlatitudes.

In summary, this experiment shows that removing the effect of the sea surface temperature gradient allows the solar radiation absorption gradient to shift the origin of the Hadley circulation southward (and weaken the Northern Hemisphere portion). The angular momentum balance is achieved through changes in the MMC momentum transports interacting with changed frictional drag. Changes in eddy transports change the eddy-induced circulation mostly in the subtropics and higher latitudes.

Experiment 2a is constructed to investigate the removal of all "external" thermal forcing by removing both the solar heating and the sea surface temperature gradient. Rainfall and evaporation do become relatively uniform with latitude (Figs. 10a, 10b) as in run 2. However, the higher heat capacity of the predominantly oceanic low latitudes and the ice and snow which are part of the initial surface conditions at high latitudes provide a weak north–south temperature gradient. As expected, the resultant MMC features a very weak Hadley circulation, confirming the central importance of the thermal gradient in forcing a Hadley circulation.

In summary, the first two experiments show that the position of the updrafts and the strength of the Hadley circulation can be related directly to the primary thermal forcing components, solar radiation absorption and sea surface temperature, which control the distribution of latent heat release. From the subtropics poleward, thermal forcing is still significant, but the structure of the circulation is influenced more by eddy heat and momentum transports.

c. *Experiment 3*

This experiment tests the complete range of hydrologic cycle effects on the MMC by suppressing evaporation from both land and ocean. After several months, precipitation is practically eliminated and cloud cover reduced by almost a factor of 2. [The model calculates cloud cover in a probabilistic fashion, so that as long as the relative humidity is not zero, it will still produce clouds. See Hansen *et al.* (1983) for more details.] The water vapor in the atmosphere decreases by more than a factor of 5. The decreased greenhouse effect, as well as the decreased poleward latent heat transport, results in high-latitude temperatures in the Northern Hemisphere about 7°C colder in January. Southern Hemisphere and equatorial temperatures are less affected because solar radiation actually reaching the surface increases with decreased cloud cover. Eddy transports of sensible heat and angular momentum are not greatly affected.

The streamfunction resulting from this experiment is shown in Fig. 14. The results, although less drastic, are similar in character to those from run 2. The lack of a competitive heat source allows the Southern Hemisphere portion of the MMC, which is driven by the gradient in radiation heating, to amplify, while the Northern Hemisphere portion of the mean circulation, no longer augmented by the latent heat release gradient, is weakened (compare Figs. 13a and 14). Changes are not as large because of offsetting changes in the gradient of the sensible heat flux from the ocean. In fact, sensible heat flux values increase to 40% of the combined latent and sensible heat flux values in the control run.

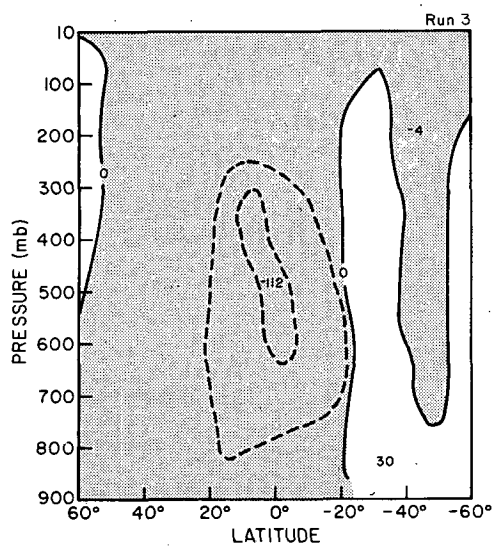

FIG. 14. Streamfunction for experiment 3.

The change of angular momentum by moist convection was reduced considerably, but it was more than compensated for by an increased effect, due to dry convection (Table 3a) in the lowest layers. However, at higher levels there was no such compensation and thus convection provided less of a frictional torque to drive poleward flow.

Elimination of evaporation reduced the thermal opacity of the atmosphere as well as eliminating the latent heating due to precipitation. To clarify the relative contribution of these two effects, two additional experiments are made. In the first (called 3a), evaporation is eliminated and the initial conditions for the run set the specific humidity in the atmosphere to zero. Thus the water vapor is completely removed from the atmosphere in contrast to the reduction of water vapor in run 3. Both runs were similar in that no precipitation occurred. The resulting streamfunction is reduced by about 40% relative to run 3, as is the sensible heat flux. The removal of atmospheric water vapor strongly affects high-latitude temperatures, so the atmospheric temperature gradient actually increases (sea surface temperatures are still specified). This result emphasizes the importance of greenhouse gases in the atmosphere for determining the strength of the Hadley circulation: without the greenhouse effect (limited basically in this run to CO_2), the ground loses heat to space by radiation and does not initiate strong atmospheric motions. With greenhouse gases, the atmospheric temperature near the surface differs from the ground temperature because of the absorption and re-emission of longwave radiation by the atmosphere. Sensible heat flux from the ground warms the near-surface atmosphere; this heating then drives a stronger mean circulation. Were all greenhouse gases to be removed from the atmosphere, it is likely that the mean circulation would be largely eliminated.

This supposition is explored in the second experiment (called 1a) in which both solar and thermal radiation were eliminated. This run is the equivalent of letting the atmosphere and surface attain local radiative equilibrium by allowing no infrared heating to take place and eliminating all shortwave absorption. With no radiative heat loss, there is no reason for the surface air temperature to be different from that of the ground, so there are no surface fluxes of heat and moisture. Without longwave radiation and heat fluxes from the specified sea surface temperature, there is no effective gradient in thermal heating (like experiment 2a). With no fluxes of moisture from the ocean the experiment dries out (like experiment 3). The streamfunction in this experiment is not significantly different from zero (the weakest in all the experiments). It should also be noted that in this experiment the momentum forcing is also removed, as expected of this "reactive" forcing, since with a greatly weakened circulation there are much weaker surface winds, surface drag and mountain drag, and without effective surface heating, convection decreases markedly. Furthermore, without radiative losses there is no reason for high latitudes to be considerably colder than low latitudes, so baroclinic instability is substantially reduced, eddy energy and transports become small, and the eddy-induced MMC is eliminated.

Experiments 1–3 and the associated experiments clearly illustrate the role of latitudinal gradients in thermal heating and the effects of greenhouse gases in driving the mean circulation. In these experiments, the various frictional forcings adjust so as to remain consistent with the altered thermal fields in their effect on the MMC. In experiments 4–6 the frictional forcing terms will be directly altered.

d. Experiment 4

In this experiment the surface drag is set to zero, eliminating the main mechanism for destroying kinetic energy in the model, especially at middle and high latitudes. The eddy kinetic energy at those latitudes increases by a factor of 3 (by a factor of 9 at low levels) and by a factor of 1.5–2 at low latitudes. Eddy transports are up to two times larger and temperatures at high latitudes increase by 10–20°C in the winter hemisphere.

The resulting Hadley circulation is shown in Fig. 15a. The low-latitude part of the circulation is weaker and the Southern Hemisphere portion has changed direction, producing a more symmetric circulation centered on the equator similar to that in experiment 1. This pattern is understandable when the altered thermal forcing pattern is examined. Fig. 16 shows the precipitation and evaporation in this experiment, as well as for the control run. Without surface friction, surface wind speeds increase by up to a factor of 6 in the NH subtropics, increasing evaporation there. The consequent rainfall provides additional thermal forcing for the subtropical portion of the Northern Hemisphere

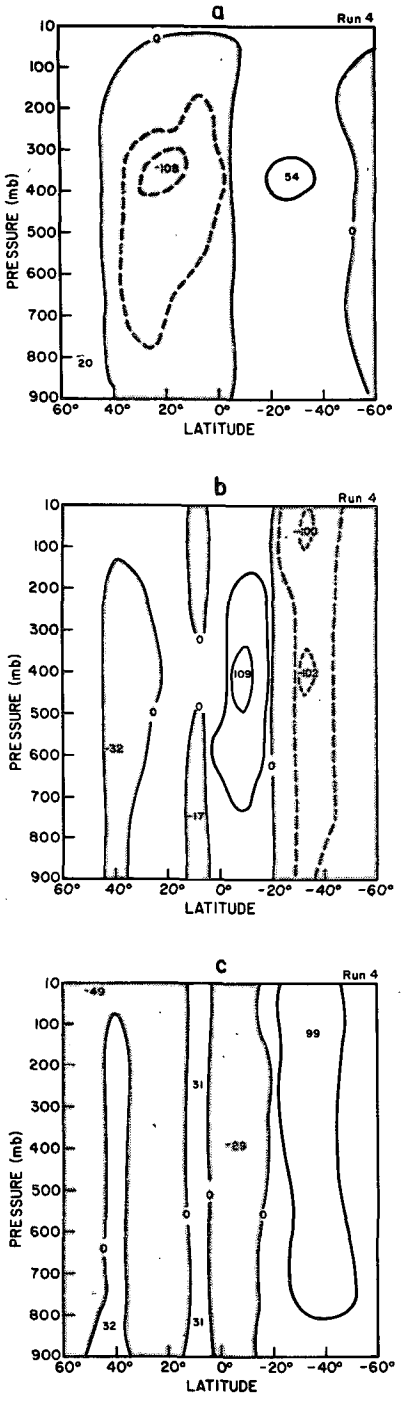

FIG. 15. As in Fig. 13 for experiment 4.

Hadley cell. The evaporated moisture also produces additional rainfall at the equator and strengthens the direct circulation in the Southern Hemisphere originating at that point. The MMC is weakened in between these two rainfall peaks. This result illustrates the interactive nature of this process: rising air associated with the upwelling branch of a meridional cell experiences greater cooling and condensation, with the subsequent latent heat release providing positive feedback on the vertical motion. Rain is more likely in the rising air and contributes to its production. Furthermore, increased surface winds and evaporation in the Northern Hemisphere subtropics result from intensified meridional circulation. In this experiment, however, all of these effects are caused by altering a momentum process rather than a thermal process, emphasizing the close coupling between the thermal and momentum forcings.

The changes in the MMC momentum balance in this experiment are also qualitatively similar to those in experiment 1. Table 3b shows the first level meridional wind and the influence of the friction terms for both the control and experiments 4–6. Note that in the control run the surface drag provides angular momentum at 16°N. In experiment 4 the loss of surface drag forcing is partially compensated by an increase in convection. The mountain torque plays a secondary role in adjusting to the new balance requirements at low latitudes in the Northern Hemisphere where it was of minor importance in the control run. The increased convection is associated with additional rainfall seen in Fig. 16a. In fact, at all tropical and subtropical latitudes where surface drag is strong in the control run, cumulus friction increases substantially in experiment 4; at latitudes in the control run where surface drag is weak, cumulus friction does not increase greatly. This illustrates the importance of cumulus convection in both the thermal budget (moist convective precipitation) and the angular momentum budget (cumulus friction) in the model.

The effects of the changed latent heat release on the transformed streamfunction are shown more clearly in Fig. 15b. The reduced precipitation in the Southern Hemisphere subtropics reduces the direct circulation (or actually augments the indirect circulation). The change in eddy contribution is shown in Fig. 15c: despite the increased magnitude of eddy transports, the distribution of convergence with height is similar to that in the control run, so differences in the induced circulation are small except at Southern Hemisphere midlatitudes, where there is a much stronger low-level heat transport associated with the strong low-level eddy kinetic energy in this experiment.

In summary, removing surface drag alters the Hadley circulation significantly, but this change results as much from the indirect effects of consequent changes in thermal forcing as from the direct momentum effects. The weakened circulation (by about 25%), shown in Table 3b, still maintains the association between the weaker drag provided by the mountains and convection and the equatorward wind in the lowest layer.

e. Experiment 5

Both surface drag and topography are eliminated; thus the surface exerts no influence on the angular

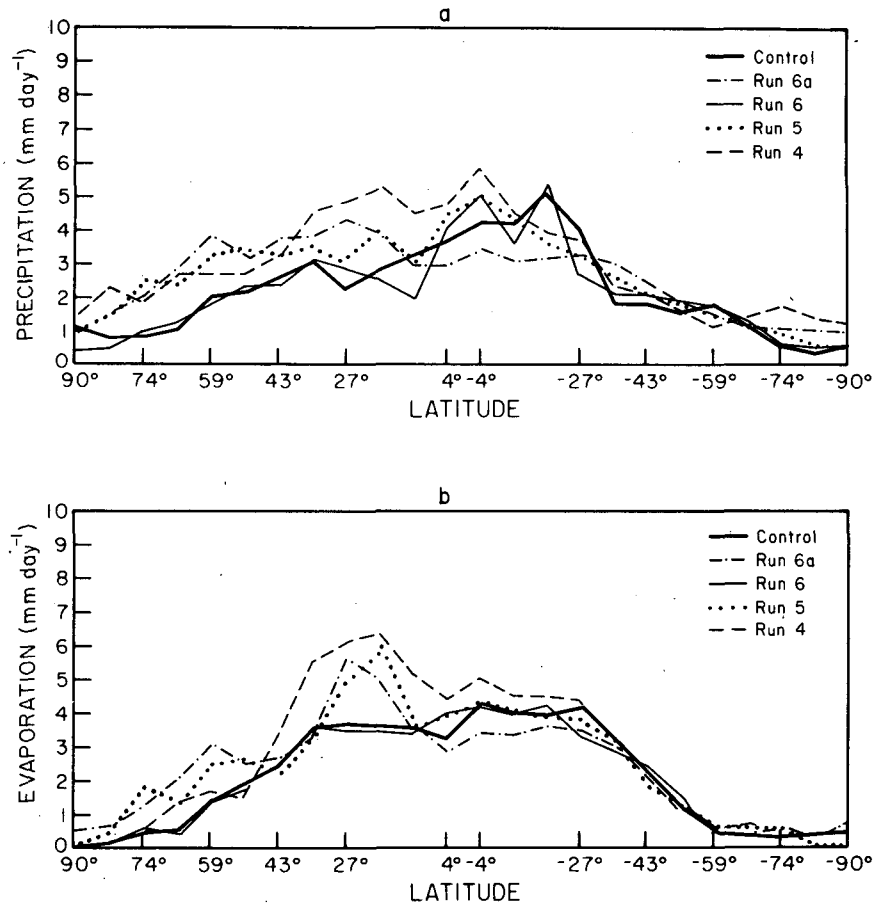

FIG. 16. (a) Precipitation and (b) evaporation as a function of latitude during January in the control run and in experiments 4–6.

momentum budget. The resulting Hadley circulation, shown in Fig. 17a, is similar to that for experiment 4. Comparison of the distributions of precipitation and evaporation (Figs. 16a,b) shows that augmentation of equatorial precipitation again occurs and is responsible for the generation of the Southern Hemisphere Hadley circulation in Fig. 17a (as in Fig. 15). However, there is now no real gradient in latent heat release from the Northern Hemisphere subtropics northward as in experiment 4; thus there is little change in the Hadley circulation from 23–39°N as in experiment 4. The transformed streamfunction change (Fig. 17b) shows this difference clearly (cf. Fig. 15b). The high-latitude response in experiment 5 seems to result from the increased latent heating there.

While eddy kinetic energy increases in the absence of surface friction, long-wave generation (especially standing waves) actually decreases without topography. Thus, while transports at low levels increase, transports at high levels, due mainly to propagating long waves, decrease. The low-level increase affects mainly latent heat transport in subtropical latitudes. Convergence of energy by eddies at these latitudes helps create direct circulation (Fig. 17c) at middle and high latitudes (cf. Fig. 15c for run 4 in which the eddies and transports are stronger at all latitudes and altitudes). These changes are augmented by the decrease in eddy angular momentum transport at high altitude. All of the alterations of the vertical distribution of momentum transports, together with the complete removal of surface effects, lead to alterations of the other momentum forcing terms in (3).

In run 4, the pressure gradient term helped counteract the loss of surface friction at Northern Hemisphere midlatitudes, but that possibility no longer exists in run 5. The changes in the angular momentum input to the first layer are shown in Table 3b. The remaining drag mechanism, convection, increases the angular momentum in the first layer, consistent with southward low-level wind. Additional significant changes in run 5 occur at 23 and 31°N and 23 and 31°S, where the mountain drag is larger in the control run. The reduced drag at these latitudes in run 5 is consistent with the weakened equatorward wind (observable at these latitudes in Fig. 17a as the weakening of the Hadley cell at low levels).

In summary, these two experiments illustrate the importance of the momentum constraints imposed on

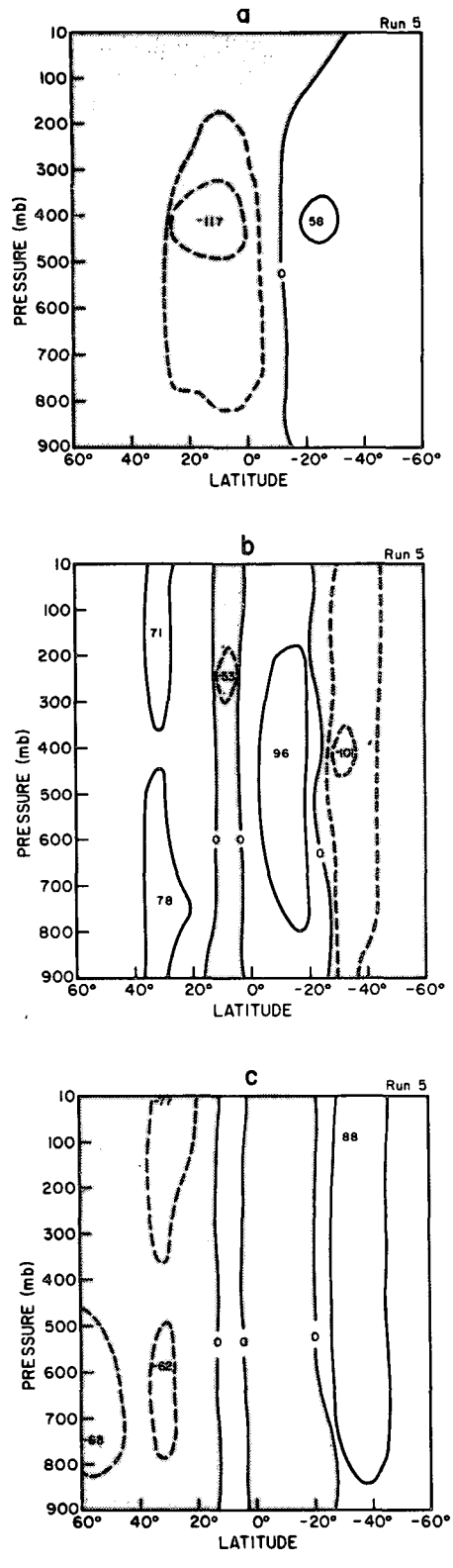

FIG. 17. As in Fig. 13 for experiment 5.

the MMC by the "reactive" surface forcing. The circulation is, however, determined by alterations of thermal forcing as well.

With the removal of the surface friction and mountain drag in experiment 5, the external torque of the planet on the atmosphere is removed. Thus the total angular momentum of the atmosphere, consisting of relative angular momentum plus planetary momentum must remain constant. This raises the question of whether the results for this experiment depend on the initial wind conditions. The planetary momentum does depend on the mass distribution in the atmosphere, but this only varies slightly from month to month with the same order of magnitude as variations in the relative angular momentum. To test the importance of the initial conditions, we started with an atmosphere (nearly) at rest in run 5a (in fact there was a slight zonal wind due to imbalances in the mass field, but the relative angular momentum is less than one-fifth of the value in run 5). The resulting streamfunction is very similar to that of run 5, with zonal wind changes featuring slightly greater east winds (relative to run 5) at low latitudes, and slightly reduced west winds at midlatitudes. The small change is understandable since the relative angular momentum of the atmosphere constitutes only about 1% of the total atmospheric angular momentum, so that even though the initial conditions had a very different wind field, the total angular momentum of the atmosphere is essentially the same. While the results of experiments like 5 and 5a certainly depend on the magnitude of the total atmospheric angular momentum (cf. experiments and discussion in Rossow and Williams, 1979), they are insensitive to changes in the initial wind field or to any changes in the initial state of the atmosphere so long as the planetary rotation rate is not changed. The effects of changes in planetary rotation were not studied here because the focus is on illustrating the potential role of the physical processes in determining the mean circulation.

f. Experiment 6

We remove only the mixing of momentum by dry and moist convection; surface drag and mountain drag are retained. In similar experiments by Helfand (1979), incorporation of momentum mixing by parameterized penetrating cumulus intensified the Hadley cell by 14%, whereas the increase was only 5% without the penetration. Stone *et al.*, (1974) found almost a 60% increase in Hadley cell intensity when they added vertical diffusivity at low latitudes to represent momentum mixing. The results shown in Fig. 18a indicate that the response of the Hadley circulation in this model is intermediate to that exhibited by the other two studies; without momentum mixing the peak circulation weakens by about 25%. The primary difference in these results is in the vertical distribution of friction [$\partial \bar{F}_x/\partial p$ in (3)]. Table 3b indicates that in the lowest model layer the angular momentum balance is maintained by surface drag and mountain drag at lower latitudes, where convection acts to remove angular momentum

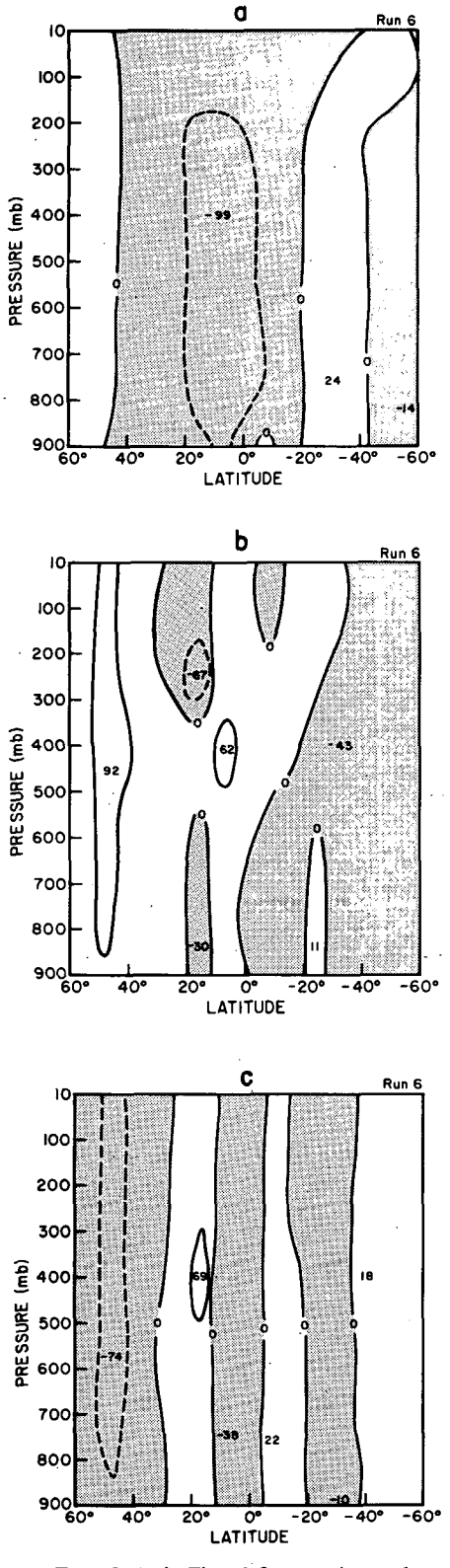

FIG. 18. As in Fig. 13 for experiment 6.

in the control run, but that these processes are inadequate to maintain strong equatorward flow in the subtropics and lower midlatitudes where convection normally deposits angular momentum by mixing with west winds aloft. Moist convection removes angular momentum at the 315 mb level in the control run; with this effect absent, poleward flow at this level diminishes strongly throughout the tropics and subtropics. The two effects combine to diminish the Hadley circulation.

Figures 16a,b give the vertically integrated rainfall and evaporation for this experiment. Not much change is evident relative to the control run, but the vertical distribution of latent heat release has changed, thereby altering the vertical structure of the MMC (Fig. 18a), mostly in the Southern Hemisphere where convection is most frequent. At 12°N there is less heating at low levels and more heating at midlevels relative to the subtropics; therefore, an indirect circulation is forced at high levels, as shown in Fig. 18b.

Without momentum mixing, eddy kinetic energy increases strongly at high levels in the tropics, but the eddy energy transports are relatively unaffected. Thus, the change in eddy effects (Fig. 18c) is relatively small at low latitudes. At midlatitudes the eddy energy is generally less affected, because momentum mixing by convection was not the main mechanism for energy destruction at those latitudes. However, convection increases by over 25%, redistributing latent heating and altering the eddy transport of sensible heat. (The heating is also changed by the altered MMC at low latitudes.) The eddy-induced mean circulation thus changes at these latitudes.

These results again illustrate that a direct change in angular momentum forcing also causes changes in those components of thermal forcing that are essentially reactive, namely, convective and eddy heat and moisture transports. Note, however, that cloud variations also alter the radiative forcing. On the other hand, when the thermal forcing was directly altered, the momentum balance changed in a reactive manner. Thus, both budgets must be considered to determine the sensitivity of the Hadley circulation to climate perturbations.

The fundamental role of momentum forcing is illustrated by an experiment (called 6a) which combines experiments 4–6. With no "external" momentum forcing, the Hadley cell in this run is substantially weaker and much narrower than in the control run. As in the previous experiments, a large equatorward wind is expected where the momentum forcing by the surface drag, mountain drag or cumulus convection adds momentum to the lowest layer (Table 3b). In this experiment, there is no momentum added by these mechanisms, so as Table 3b indicates, the wind is small everywhere except near the equator. In this region the Coriolis parameter is very small; consequently, without the friction terms, a large meridional velocity is forced by the thermal forcing gradient without upsetting the balance in Eq. (6).

The important point is that, with the geostrophic constraint on Earth's circulation away from the equa-

TABLE 4a. Northern Hemisphere Hadley cell characteristics.

Experiment	N Limit	S Limit	Peak circulation intensity (10^9 kg s^{-1})	Peak latitude	Peak pressure (mb)	Pressure of −10 contour (mb)	Latitudinal extent	Peak intensity and latitude of Ferrel cell	Eddy kinetic energy at 39°N* (10^4 J m^{-2})	Latitude of peak rainfall
Control	47°N	16°S	125	8°N	400	236	63	13/55°	105	20°S
1	39°N	8°N	198	16°N	400	236	31	16/55°	175	12°N
2	63°N	31°S	80	8°N	400	236	92	11/70°	48	27°S
3	55°N	16°S	112	8°N	400	400	71	11/63°	80	—
4	39°N	0	108	23°N	400	236	39	20/47°	328	4°S
5	63°N	8°S	117	8°N	400	236	71	1/70°	247	4°S
6	39°N	16°S	99	8°N	400	100	55	17/63°	124	20°S

* Peak intensity.

tor, the meridional circulation *must* be consistent with *both* the thermal and frictional forcing. Experiments 1a, 2a and 6a show that when either thermal or frictional forcing is entirely removed, the circulation away from the equator must go to zero.

5. Discussion

Table 4 summarizes the major changes in the model Hadley circulation for the experiments by showing among other things, the northern and southern limits, the peak streamfunction intensity, and the location of peak streamfunction intensity. In the following discussion we review the same experiments previously discussed to highlight the processes that influence particular features of the MMC. The cell limits are determined by the latitudes between which the vertically integrated streamfunction is negative (positive for the Southern Hemisphere); no interpolation is made to avoid spurious variations. In the control run there are no year-to-year variations in the cell limits. The last three columns give the Ferrel cell peak intensity, the vertically integrated eddy kinetic energy, and the latitude of maximum precipitation (in Table 4a only, as it applies to both hemispheres).

a. Equatorward limit

The latitudinal extent of the Hadley circulation in these experiments depends on the location of sources and sinks of heat and angular momentum and on the relative intensities of the Hadley and Ferrel circulations. In the control run the January Hadley circulation streamfunction appears to be a dipole-like pattern caused by a source of heat located near 20°S, coinciding with a maximum of precipitation. In addition, a source of momentum at the surface near 12°N, coinciding with the maximum westerly drag induced by the surface drag and topography, reinforces the Northern Hemisphere cell. In the Southern Hemisphere, the surface drag and topography partially cancel each other, providing only weak momentum forcing for the Southern Hemisphere Hadley circulation (see Table 3a).

The variations in direct heating distribution in experiments 1 and 2 correlate with variations of the equatorward limit of the Hadley cells and the location of maximum precipitation (Table 4 and Fig. 10a). In the control run, the combination of solar radiation and sensible heat flux from the surface (where ocean temperatures are specified) leads to a maximum heating near 27°S, but latent heating effects shift the maximum to 20°S (Fig. 10a). Maximum mean vertical velocities

TABLE 4b. Southern Hemisphere Hadley cell characteristics.

Experiment	N Limit	S Limit	Peak circulation intensity (10^9 kg s^{-1})	Peak latitude	Peak pressure (mb)	Pressure of −10 contour (mb)	Latitudinal extent	Peak intensity and latitude of Ferrel cell	Eddy kinetic energy of 39°N* (10^4 J m^{-2})
Control	16°S	39°S	63	31°S	400	236	23	17/55°	67
1	8°S	39°S	120	16°S	400	236	31	10/55°	93
2	39°S	47°S	25	39°S	400	400	8	1/47°	16
3	23°S	39°S	30	31°S	884	400	16	4/39°	57
4	8°S	47°S	54	23°S	400	236	39	15/70°	162
5	16°S	63°S	58	23°S	400	236	47	None	120
6	23°S	39°S	24	31°S	741	236	16	14/55°	76

* Peak intensity.

also occur at the same latitude (Fig. 1d). In experiment 1, with only the specified sea surface temperature providing forcing, the evaporation maximum shifts into the Northern Hemisphere near the peak in zonal mean sea surface temperatures, and the rainfall peak shifts near to the equator. This location then becomes the origin for circulations spiraling away in both hemispheres. In experiment 2, with only solar heating which peaks near 35°S (Fig. 9), the latent heating shifts the maximum in precipitation to 27°S. Consequently, the direct cell streamfunction extends to 31°S (Fig. 13a). This correlation in behavior between peak heating, evaporation, precipitation, and the location of the equatorward limit of the Hadley circulations is a consequence of a kind of CISK feedback between the MMC and latent heating. Any external heating (solar or surface sensible heat) drives vertical motions and near surface horizontal convergent flow. Stronger surface winds increase evaporation and concentrate the moisture in the updraft region. The consequent latent heating occurs both in large-scale condensation (Fig. 2b) and moist convection (Fig. 2d). This additional latent heating serves to concentrate the total heating more strongly in latitude and drive a stronger Hadley circulation (cf. experiment 3). In experiment 2a, with no solar heating or gradient in sea surface temperature, the latent heating is nearly uniform with latitude (Fig. 10a) and the mean circulation is very weak (there is still a weak gradient in heating produced by latitudinal variations in land fraction and remnant polar ice from the initial surface conditions). All of these results, together with the observed seasonal variation of the equatorward limit (represented in these experiments by a comparison of Northern Hemisphere and Southern Hemisphere circulations), suggest that the equatorward limit on the Hadley circulation is controlled primarily by the latitudinal location of the maximum *total* heat source. The total heat source location is modified by the nonlinear latent heat effects interacting with the dynamic motions which the radiative and surface heat sources drive.

The equatorward limit is less affected by changes in the momentum forcing, but stronger surface winds lead to more evaporation and condensation which can alter the equatorward limit somewhat (e.g., experiment 4). However, when all the momentum forcing is eliminated, the circulation is confined to the equator (experiment 6a) regardless of the thermal forcing, so that the balance in Eq. (6) may be maintained (see Table 3b).

b. *Poleward limit*

The location of the poleward limit of the Hadley circulation in these experiments depends on the relative intensities of the forcing for the Hadley and Ferrel circulations. (Since the planetary rotation rate is not changed and the static stability changed little for most experiments, variation of Hadley cell extent is not due to changes in inertial or static stability.) The primary forcing for the MMC in subtropical and midlatitudes is provided by eddy heat and momentum transports. Schneider and Lindzen (1977) and Taylor (1980) interpreted their model results to imply control of the poleward limit of the Hadley circulation and creation of the Ferrel circulation solely by eddy momentum transports; however, these interpretations depend heavily on the parameterization of eddy transports employed in those models and contradict diagnostic studies that show both heat and momentum transports playing important roles (Vernekar, 1956; Crawford and Sasamori, 1981; Pfeffer, 1981; see also Kuo, 1956). Fig. 7 compares the different eddy forcing terms in Eq. (3) for the control run at northern midlatitudes. (The vertical transport convergences are in general some four orders of magnitude less than the horizontal ones, so they are ignored.) The momentum and the sensible heat transports by eddies appear to force mean circulations of the same order of magnitude, in this case helping to generate a Ferrel cell between 40–60°N. [A similar comment applies to the Southern Hemisphere, but as noted by Pfeffer (1981) the relative strength of the eddy heat and momentum forcing changes seasonally, with momentum forcing dominant in summer.] Since the eddies in midlatitude are generated primarily by baroclinic instability and are also responsible for moisture transport and large scale cloudiness, the response of the MMC in this region to climate perturbations may be quite complex.

Experiments 1, 4 and 6 all exhibit equatorward shifts of the poleward limit of the Northern Hemisphere Hadley circulation, whereas the poleward limit of the Southern Hemisphere Hadley cell remains the same or shifts poleward (in experiment 4). These changes can be understood from the differences in the changes of Hadley and Ferrel cell intensity (Table 4). The eddy kinetic energy increased in all these experiments, suggesting that increased eddy transports are responsible for changing the relative balance of Hadley and Ferrel circulations. The increased land–ocean temperature contrast, caused by removing solar heating in experiment 1, not only provides greater forcing for standing eddy motions, but also strengthens their heat flux divergence/convergence in northern midlatitudes. This effect is less important in the Southern Hemisphere, so little change occurs. The pattern of $\partial\bar{G}/\partial y$ in (3) leads to an increase in the Ferrel circulation that more than offsets an increase in the Hadley circulation (Fig. 12b) and shifts the dividing line equatorward. In experiment 4, the removal of surface drag also leads to an increased eddy energy and eddy heat divergence/convergence (Fig. 15c) which weakens the Northern Hemisphere Hadley cell relative to the Ferrel cell (Table 4). In addition, the eddy contribution to $\partial\bar{L}/\partial p$, plus topographic effects providing surface forcing through $\partial\bar{F}_x/\partial p$, helps maintain the Ferrel cell intensity. In the

Southern Hemisphere, the weaker topographic forcing is unable to offset the removal of surface drag leading to a weaker Ferrel cell and a poleward shift of the southern limit. In experiment 6, the vertical mixing of momentum by convection is removed. Since this is a major dissipation process in the model, eddy kinetic energy again increases. The altered eddy heat and momentum convergences (Fig. 18c) weaken the Hadley cells and strengthen the Northern Hemisphere Ferrel cell, shifting the dividing line equatorward. In addition, the Ferrel cell generation is made more effective as the angular momentum forcing is confined more in altitude (see the discussion in Section 2). The Southern Hemisphere response is explained more by the change in the vertical distribution of angular momentum forcing caused by removing convection than by the changed horizontal eddy transport magnitudes. In this case the peak intensity of the Hadley cell shifts to a much lower altitude, but the relative strengths of the Hadley and Ferrel cells at this altitude are still nearly the same as in the control run. Consequently, the boundary between the cells does not shift.

Experiments 2, 3 and 5 exhibit poleward shifts of the poleward limit of the Hadley circulation. When topography and surface friction are removed as in experiment 5, explicit forcing for the propagating long waves is removed. This change, despite an increase in total eddy kinetic energy, weakens the heat and momentum convergence, especially at higher altitudes. In addition, there is no longer a surface sink for westerly momentum mixed downward by convection. These two changes lead to substantially diminished Ferrel cells (Fig. 17). Consequently, the poleward limit of the Hadley cells moves farther poleward than in any other experiment. In experiments 2 and 3, eddy kinetic energy decreases making $\partial \bar{H}/\partial y$ more important than $\partial \bar{G}/\partial y$ and reducing $\partial \bar{L}/\partial p$ for the Ferrel cell. A qualitatively similar shift occurs in summer along with a weakening of $\partial \bar{H}/\partial y$. The alterations in the total heating (Figs. 13 and 14), caused by the changed hydrologic cycle, also shift the center of the Ferrel cell poleward allowing the Hadley cell to extend farther poleward (Table 4).

c. *Vertical extent*

The vertical extent of the Hadley cells, as indicated by the location of the peak intensity and a reference contour value, is essentially constant in altitude for all experiments except 3 and 6. The relatively coarse vertical resolution, and the lack of substantial alteration in the static stability, presumably lead to this result. In experiment 3 where all water is removed, the static stability decreased in the lower troposphere as the atmospheric lapse rate shifted toward dry adiabatic, while the upper troposphere became relatively more stable. Although the peak intensity location in the Northern Hemisphere cell does not shift, the extent of the Hadley circulation above the peak decreases (Fig. 14). The change in the vertical extent in the Northern Hemisphere implied by Table 4 for experiment 6 is not significant (see Figs. 1f and 15a). However, the changes occurring in the Southern Hemisphere Hadley cell in experiments 3 and 6 both show that the vertical mixing of momentum by penetrating convection plays a role in determining the vertical extent. The effect is strongest in the Southern Hemisphere because more moist convection occurs there in January.

d. *Peak intensity*

The peak streamfunction intensity in these experiments is a function of the magnitude and coherency of the thermal forcing, although the frictional forcing and eddy transports are also influential. The gradient of heating due to latent heat release is revealed in the rainfall distribution (Fig. 10a) which also tends to mark the location of Hadley cell updrafts. In most of these experiments the latitudinal distribution of rainfall is more uniform than in the control run, and the Hadley cell intensity is reduced (Table 4). Only in experiment 1 is the rainfall more sharply localized, resulting from the removal of the competition between solar heating and sea surface temperature forcing, which peak at different latitudes for January (Fig. 9). The fact that a uniform sea surface temperature in experiment 2 did not lead to a strong rainfall peak near the latitude of strongest solar heating suggests that the effect of sea surface temperatures on evaporation is more important in determining the location of the rainfall maximum than is direct solar radiation absorption (although one must bear in mind that the specified sea surface temperatures actually occur in response to forcing by radiation and surface winds). Indeed, the rainfall maximum in the control run, with both solar heating and a proper sea surface temperature distribution, is at a latitude between the peak of the solar heating and sea surface temperature maximum. The consequence of a more coherent heating distribution in run 1 is a stronger circulation. In run 2a, with the removal of both the sea surface temperature gradient and solar radiation, the mean circulation is very weak, illustrating the essentially "reactive" nature of the latent heat forcing.

Experiment 3 further illustrates the amplifying effects of water processes. The MMC is similar to that in the control run, but slightly weaker (Fig. 14 and Table 4). The decrease in total heating gradient, caused by removal of latent heating, is offset by increased solar heating of land without cloud cover and increased sensible heat flux from the ocean, coupled with decreased poleward total heat flux by eddies. The former compensation is less effective in the Southern Hemisphere where land fraction is smaller and air temperature warmer, producing a larger decrease in the Southern Hemisphere Hadley cell intensity. Thus, while the la-

tent heat effects in this model only slightly enhance the intensity of the Hadley circulation, they actually make the circulation more efficient at transporting heat, producing a smaller equator-to-pole temperature gradient for the same radiative forcing and MMC intensity.

At the same time, water vapor makes radiation less efficient at removing heat, as illustrated in experiments 1a and 3a. In experiment 3a, with no atmospheric water vapor, the Hadley circulation was reduced by 40% from that of run 3, despite a much stronger thermal gradient. In run 1a, with no longwave or shortwave radiation (but still a gradient in sea surface temperatures) the Hadley cell essentially disappears. When the atmosphere loses the ability to absorb radiation coming from the ground, and thus maintain a temperature gradient between the surface air temperature and the ground temperature, there is no effective way for the ground to transmit its energy to the atmosphere (by latent or sensible heat). In the absence of atmospheric opacity, the radiation goes straight out to space. Under these conditions the mean circulation is independent of the latitudinal temperature gradient, which only depends on the magnitude of the radiative forcing.

Reduction of frictional forcing, as in experiments 4–6, also diminishes the Hadley cell intensity somewhat (Tables 4a,b). Part of this effect is caused by increased eddy kinetic energy which augments high-latitude precipitation (Fig. 16), thereby diminishing the gradient in total thermal heating. As the frictional forcing and thermal forcing of the mean circulation must be consistent, a net alteration in the frictional forcing, such as altering the momentum mixing by penetrating convection, will result in an alteration in thermal forcing and a change in the mean circulation. In experiment 6a, when all momentum forcing is removed, the Hadley circulation is much less intense and is confined to the equator where the balance in (6) can still be maintained.

6. Conclusions

The aim of this paper is to present a series of experiments which highlight the interactions of the Hadley circulation in a system with many feedbacks like the Earth's atmosphere. The model Hadley circulation responds to perturbations in both the thermal and momentum forcing, but a clear distinction between these two types of perturbations cannot be made because of the coupling between these two budgets. This coupling is often mediated by "small" terms in the equations of motion which are neglected in simpler analyses. Examination of Table 4 suggests two points. 1) The adjustments among the many processes forcing the Hadley circulation are generally able to compensate for removal of a single process. This illustrates the potential complexity of Hadley circulation adjustments to climate changes. 2) The extreme experiments which remove all of one kind of forcing suggest, nevertheless, that the first-order structure of the Hadley circulation is produced by the "external" thermal and momentum constraints, which may explain why simpler models with adjustable parameters can usually obtain realistic Hadley circulations. The small changes which do occur in the single-process experiments would be considered climatologically significant, however, so that consideration of the precise thermal and momentum balances, modified by many processes, is required to determine the sensitivity of the Hadley circulation to climate perturbations and the precise form which the response takes. Consequently, no process can be left out of a model if a determination of a realistic response of the Hadley circulation is desired, particularly a realistic account of the differences in sensitivity between the Northern and Southern Hemispheric, summer and winter Hadley circulations.

These experiments indicate that changes in Hadley circulation associated with climate perturbations will be connected with the following processes: 1) change in location, magnitude or timing of solar insolation maximum, as might occur due to Milankovitch (orbital) effects, cloud cover changes, or surface albedo (vegetation) changes; 2) change in sea surface temperature patterns, which may result from altered solar heating, altered surface winds, or altered ocean dynamics (both vertical and horizontal); 3) change in evaporation and latent heat release, due to changes in atmospheric temperature, stability and surface wind field; 4) change in surface friction, associated with surface wind and static stability; 5) change in topography, which occurs over geologic time periods; 6) change in convection and convective mixing of momentum, associated with atmospheric stability, temperature and moisture content; and 7) change in baroclinicity and eddy characteristics. This last item includes changes in the wavelength and thus the vertical propagation ability of eddies and changes in third-order quantities such as the horizontal and vertical gradients of eddy heat and momentum flux divergence.

To properly simulate Hadley cell changes associated with particular climate perturbation mechanisms, it is necessary to simulate properly the above processes. This may be beyond the capability of current models. Processes 1), 3) and 6) demand realistic modeling of clouds, condensation and convection; processes 3) and 4) require realistic surface and boundary layer turbulence; process 2) requires a realistic mixed-layer ocean or ocean dynamics model; processes 5) and 7) indicate the necessity for using global models (as opposed to sector models); and process 7) requires sufficient horizontal and vertical resolution, as well as proper longwave generation, to account properly for eddy energy, momentum and moisture transports. This analysis suggests that the shifting arid zones predicted by some current models for increasing CO_2 must be viewed with caution. The same can be said for any regional climate characteristic that depends on the

Hadley circulation. The Hadley cell is sensitive to numerous processes and interactions that can produce small changes with large consequences for human society. Accurate prediction of such small variations represents a challenge for atmospheric modelers.

Acknowledgments. The authors thank R. Suozzo for computer assistance, A. Del Genio, L. Travis and W. Robinson for their helpful comments and I. Held for his useful comments in review. This work was supported by the National Aeronautics and Space Administration Climate Program Office managed by Dr. R. A. Schiffer.

REFERENCES

Crawford, S. L., and T. Sasamori, 1981: A study of the sensitivity of the winter mean meridional circulation to sources of heat and momentum. *Tellus,* **33,** 340–350.

Dickinson, R., 1971: Analytic model for zonal winds in the tropics. *Mon. Wea. Rev.,* **99,** 501–510.

Dunkerton, T., 1978: On the mean meridional mass motions of the stratosphere and mesosphere. *J. Atmos. Sci.,* **35,** 2325–2333.

Eliassen, A., 1951: Slow thermally or frictionally controlled meridional circulation in a circular vortex. *Astrophys. Norv.,* **5,** 19–60.

Gallimore, R., and D. Johnson, 1981: The forcing of the meridional circulation of the isotropic zonally averaged circumpolar vortex. *J. Atmos. Sci.,* **38,** 583–599.

Gilman, P., 1964: On the mean meridional circulation in the presence of a steady state, symmetric, circumpolar vortex. *Tellus,* **16,** 160–167.

Hansen, J., G. Russell, D. Rind, P. Stone, A. Lacis, S. Lebedeff, R. Ruedy and L. Travis, 1983: Efficient three dimensional global models for climate studies: Models I and II. *Mon. Wea. Rev.,* **111,** 609–662.

Held, I. M., and A. Y. Hou, 1980: Nonlinear axially symmetric circulations in a nearly inviscid atmosphere. *J. Atmos. Sci.,* **37,** 515–533.

Helfand, H. M., 1979: The effect of cumulus friction on the stimulation of the January Hadley circulation by the GLAS model of the general circulation. *J. Atmos. Sci.,* **36,** 1827–1843.

Holton, J. R., 1975: *The Dynamic Meteorology of the Stratosphere and Mesosphere, Meteor. Monogr.,* No. 37, Amer. Meteor. Soc., 216 pp.

Hunt, B. G., 1973: Zonally symmetric global general circulation models with and without the hydrologic cycle. *Tellus,* **25,** 337–354.

——, 1979: The influence of the Earth's rotation rate on the general circulation of the atmosphere. *J. Atmos. Sci.,* **36,** 1392–1408.

Kuo, H. L., 1956: Forced and free meridional circulations in the atmosphere. *J. Meteor.,* **13,** 561–568.

Lau, K., 1979: A numerical study of tropical large-scale air-sea interaction. *J. Atmos. Sci.,* **36,** 1467–1489.

Manabe, S., and R. T. Wetherald, 1980: On the distribution of climate change resulting from an increase in CO_2 content of the atmosphere. *J. Atmos. Sci.,* **37,** 99–118.

Oort, A. H., and E. Rasmusson, 1971: *Atmospheric Circulation Statistics.* NOAA Prof. Pap. 5, U.S. Dept. Commerce, 323 pp.

Pfeffer, R. L., 1981: Wave-mean flow interactions in the atmosphere. *J. Atmos. Sci.,* **38,** 1340–1359.

Rossow, W. B., 1983: A general circulation model of a Venus-like atmosphere. *J. Atmos. Sci.,* **40,** 273–302.

——, and G. P. Williams, 1979: Large-scale motions in the Venus stratosphere. *J. Atmos. Sci.,* **36,** 377–389.

Salustri, G., and P. H. Stone, 1983: A diagnostic study of the forcing of the Ferrel cell by eddies, with latent heat effects included. *J. Atmos. Sci.,* **40,** 1101–1109.

Schneider, E. K., and R. S. Lindzen, 1977: Axially symmetric steady-state models of the basic state for instability and climate studies. Part I: Linearized calculations. *J. Atmos. Sci.,* **34,** 263–279.

Schoeberl, M. R., and D. F. Strobel, 1978: The zonally averaged circulation of the middle atmosphere. *J. Atmos. Sci.,* **35,** 577–591.

Stone, P. H., W. J. Quirk and R. C. J. Somerville, 1974: The effect of small-scale vertical mixing of horizontal momentum in a general circulation model. *Mon. Wea. Rev.,* **102,** 765–771.

Taylor, K. E., 1980: The roles of mean meridional motions and large-scale eddies in zonally averaged circulations. *J. Atmos. Sci.,* **37,** 1–19.

Vernekar, A. D., 1967: On mean meridional circulations in the atmosphere. *Mon. Wea. Rev.,* **95,** 705–721.

Williams, G. P., and J. L. Holloway, 1982: The range and unity of planetary circulations. *Nature,* **297,** 295–299.